IEEE Access
Multidisciplinary | Rapid Review | Open Access Journal

Received 5 December 2023, accepted 28 December 2023, date of publication 9 January 2024,
date of current version 19 January 2024.

Digital Object Identifier 10.1109/ACCESS.2024.3351715

THEORY

A Simplified Electrical-Based Model for Electroporation Dynamics

AMANDA M. LOVELESS[1], (Member, IEEE), SAMUEL J. WYSS[1], (Graduate Student Member, IEEE), WILLIAM MILESTONE[2], RAVI P. JOSHI[2], (Fellow, IEEE), AND ALLEN L. GARNER[1,3,4], (Senior Member, IEEE)

[1]School of Nuclear Engineering, Purdue University, West Lafayette, IN 47907, USA
[2]Department of Electrical and Computer Engineering, Texas Tech University, Lubbock, TX 79409, USA
[3]Elmore Family School of Electrical and Computer Engineering, Purdue University, West Lafayette, IN 47907, USA
[4]Department of Agricultural and Biological Engineering, Purdue University, West Lafayette, IN 47907, USA

Corresponding author: Allen L. Garner (algarner@purdue.edu)

This work was supported by the Office of Naval Research under Grant N00014-21-2055.

ABSTRACT Calculating pulsed electric field (PEF)-induced pore formation using the Smoluchowski equation (SME) can be computationally expensive, even when reduced to the asymptotic SME (ASME). These issues are exacerbated when incorporating additional physical phenomena, such as membrane temperature gradients or shock waves, or incorporating pore formation into multiscale models starting from an external stimulus at the organism level. This study presents a rapid method for calculating the membrane-level effects of PEFs by incorporating a semi-empirical equation for transmembrane potential (TMP)-dependent membrane conductivity into a single-shell model for calculating the TMP. The TMP calculated using this approach and the ASME agreed well for a range of electric field strengths for various PEF durations and AC frequencies below and above the threshold for pore formation. These results demonstrate the feasibility of rapidly predicting TMP, which is easily measured, during pore formation strictly from electrical properties and dynamics without needing to explicitly calculate pore dynamics, as required when using the SME and ASME.

INDEX TERMS Bioelectrics, electroporation, Laplace's equation, Smoluchowski equation, transmembrane potential.

I. INTRODUCTION

Pulsed electric fields (PEFs) have been used for various medical and biological applications [1], [2], [3] for decades after the initial demonstration of PEF-induced microorganism inactivation [4], [5], [6]. Some applications include food shelf-life extension [7], [8], [9], [10], [11], [12], [13], [14], [15], [16], [17], [18], cell permeabilization for gene therapy and chemotherapeutic drug delivery optimization [19], [20], [21], [22], [23], [24], [25], [26], [27], [28], ex-vivo platelet activation to enhance wound healing [29], [30], [31], synergistic combinations with other technologies for microorganism inactivation [6], [14], [32], [33], [34], cardiac ablation [35], [36], [37], [38], extraction of valuable intracellular materials (e.g., lipids from microalgae) [39], [40], [41], [42], [43], [44], [45], [46], [47], [48], [49], [50], [51], [52], [53], [54], [55], [56], and targeted cancer treatment through irreversible electroporation [57], [58], [59], [60], [61], [62], [63], [64], [65] or apoptosis induction [23], [67], [68]. PEFs can also block (or induce) action potentials across nerves [69]. While physical, chemical, and pharmacological approaches can achieve the same result [70], [71], electrical stimulation is attractive because it provides rapidness and reversibility. The ability to propagate or arrest action potentials with PEFs is useful for pain mitigation [72], [73] and nonlethal defense.

Electroporation, which occurs when the applied PEF sufficiently increases the transmembrane potential (TMP) to allow for pore formation [3], [74], [75], is crucial for these applications. Upon removing the electrical stimulus, the

The associate editor coordinating the review of this manuscript and approving it for publication was Mahmoud Al Ahmad.

resulting pores may either reseal (reversible electroporation), which may facilitate molecular or drug transport into the cells to modify cellular function, or continue to grow (irreversible electroporation), which leads to cell rupture and death, often through necrosis [75]. Generally, pulse durations shorter than the charging time of the membrane (typically hundreds of nanoseconds to 1 μs) do not sufficiently charge the membrane to induce conventional electroporation [76], [77]. Instead, they require stronger applied electric fields and often generate a larger number of smaller pores [3], [78], [79], [80], [81], which may still be sufficiently large to allow ions into the cell for applications such as blocking action potentials across nerves [82] or permitting calcium transport for platelet activation [31]. Moreover, even applying trains of such nanosecond PEFs (nsPEFs) only increases the number of pores, but not the size [83]. While their duration may prohibit fully charging the cell membrane, such nanosecond PEFs (nsPEFs) can charge intracellular structures to induce changes in cellular function, such as calcium release or apoptosis [72].

To properly assess the PEF parameters necessary for these applications, robust theoretical models have been developed to assess pore dynamics [3], [74], [84]. The most common approach is the Smoluchowski equation (SME) [74], which gives the probability density function $n(r,t)$ denoting the number of pores per unit area with radii between r and $r+dr$ at an instantaneous time t [85]. While the SME elucidates the dynamics of pore number and size following PEFs, it requires solving a partial differential equation, given by [86]

$$\frac{\partial n}{\partial t}+D\frac{\partial}{\partial r}\left(-\frac{1}{kT}\frac{\partial \varphi}{\partial r}n-\frac{\partial n}{\partial r}\right)=S(r), \tag{1}$$

where D is the diffusion constant of pores, $\varphi(r)$ is the pore energy, k is the Boltzmann constant, T is the absolute temperature, and $S(r)$ is the source term that represents the creation and destruction of pores [86]. Neu and Krassowska [86] outlined several challenges with solving this equation, including its reliance on many parameters that could not be measured directly, the difficulty in relating these constants to measured values, and computational challenges introduced by the exponential terms in the pore creation. They performed an asymptotic analysis to reduce the SME to an ordinary differential equation with fewer parameters and improved computational efficiency. This is especially valuable when trying to link pore formation to other physical phenomena. For instance, Joshi et al. [69] developed a self-consistent theory for action potential behavior in a neuron exposed to a PEF by incorporating the shunt conductance resulting from the pore dynamics determined using this asymptotic Smoluchowski equation (ASME) with the standard cable model for a neuron [87]. It also allows assessing electroporation dynamics for more realistic multiscale systems using commercial software (e.g., COMSOL Multiphysics) by reducing the computational expense that would be required by the full SME [88]. While reducing the PDE to an ODE makes the ASME much more computationally inexpensive than the SME, the ASME still requires tracking the pore number and pore size, which becomes prohibitive for the shorter pulse durations due to the large number of small pores generated [80], [81].

Increasingly, PEF-induced bioeffects require accounting for multiphysics and multiscale phenomena. For instance, Goldberg et al. coupled Poisson's equation, the Nernst-Planck equations for ion motion, membrane deformation, and the SME to assess membrane permeabilization [89]. Multiphysics modeling coupling the SME with the Nernst-Planck model have also examined bioeffect cancellation due to bipolar PEFs [90]. More realistic multiphysics models have included three-dimensional models using the ASME to probe electroporation in irregularly shaped cells [91], arrays of multiple cells [92], and cells that undergo PEF-induced deformation [93], [94]. The computational expense increases with the incorporation of additional physical phenomena. Moreover, the computational expense increases by incorporating phenomena across multiple length scales. One example is assessing skin electroporation by assessing the electric field effects and diffusion from length scales ranging from the skin to an individual membrane by using molecular dynamics [95]. Weinert et al. developed dynamic, multiphysics simulations of electroporation of various tissues in rabbits, although they did not assess the dynamics of electroporation at the pore level [96]. In addition to PEFs, RF and microwave radiation may also penetrate the body and induce multiphysics phenomena that may influence TMP and cellular function [97].

This study seeks to avoid this computational difficulty by developing a strictly electrical-based approach to modeling electroporation dynamics without directly calculating the pore dynamics. We accomplish this by combining a semi-empirical relationship between cell membrane conductivity and TMP [98] with a system of equations used to calculate TMP [99] to calculate TMP self-consistently during various electromagnetic waveforms (both PEFs and AC fields) without needing to directly calculate pore density. We achieve excellent agreement between this TMP-based approach and the ASME with minimal computational expense. This approach would allow for rapid coupling with other physical phenomena, such as membrane temperature gradients [100], or coupling with multiphysics software, such as Sim4Life or COMSOL Multiphysics [88], to assess multiscale effects from the organism to membrane level.

Section II presents the derivation of the simplified electrical-based electroporation model. We compare this simplified model to the ASME for various square PEFs, sinusoidal fields, and exponential fields in Section III. We discuss the differences in the models and remark on future analyses using the simple model in Section IV. Section V provides concluding remarks.

II. MODEL DERIVATION

In ASME models [86], the TMP is calculated explicitly at each timestep using a finite difference approach based

on the conservation of energy, current density, and electric flux where applicable. Throughout this study, we follow the implementation of the ASME from Talele et al. [101]. Instead of the full SME, the ASME solves

$$\frac{dN}{dt} = \psi e^{(\Delta\Phi_m/V_{ep})^2}\left(1 - \frac{N}{N_{eq}}\right), \tag{2}$$

where ψ is the pore creation rate coefficient, $\Delta\Phi_m$ is the TMP evaluated at time t, V_{ep} is the characteristic voltage of electroporation, and N_{eq} is the equilibrium pore density, which is a function of $\Delta\Phi_m$ [101]. Using the TMP, (2) can be solved directly by linearization to provide the net change to the pore density from which individual pores are created. The radius r_q of a given pore is updated at each timestep by linearizing

$$\frac{dr_q}{dt} = -\frac{D}{kT}\frac{\partial w_m}{\partial t}, \tag{3}$$

where D is the diffusion coefficient for pores and w_m is the lipid bilayer energy [101].

Pores can drastically change the electrical properties of the membrane by changing the amount of water in the membrane (which changes the membrane permittivity) and facilitating the passage of ions across the membrane (which alters the membrane conductivity). A useful measure of the overall degree of the relative poration of a membrane is the fractional pore area (FPA). For q pores, FPA is given by

$$\rho_p = \frac{\pi}{A_m}\sum_q r_q^2, \tag{4}$$

where A_m is the area of the membrane or a segment of the membrane if radial effects are considered. Equation (4) can be used to update σ_m at each timestep by considering the fractional pore area as a weighted average of the conductivities of the suspension σ_s and sealed plasma membrane σ_{pm} as

$$\sigma_m = \sigma_s\rho_p + \sigma_{pm}\left(1 - \rho_p\right). \tag{5}$$

These models generally track and evolve pores on an individual basis. Thus, it is necessary to individually update and manage pore distributions containing approximately 10^3-10^8 pores at each of the 10^3-10^4 discrete time steps.

The management of pores in these models generally consumes the majority of model runtime, especially when many small pores are created, such as for nsPEFs with high electric field strengths. Several computational optimizations can be used, such as managing pores that form nearby temporally and spatially as groups [101], which can reduce the number of pore variables that need to be managed. However, the choice of the size of these groups is somewhat arbitrary, making it difficult select an optimal "group size" that effectively reduces the number of operations needed to maintain pores without significantly altering pore evolution dynamics. Additionally, pore management can be sped up by using process and/or instruction level parallelism, which can reduce the amount of time required to manage pores at the cost of additional model complexity. While both methods can dramatically speed up ASME models, neither can eliminate the computational load of managing pores individually.

While the ASME is more computationally efficient than the SME, which provides the most fidelity for pore dynamics, it is still computationally expensive for performing parametric analyses, particularly when pore densities increase dramatically, which occurs for PEFs with short durations and strong electric fields. Moreover, from a practical perspective, experimentalists often do not specifically measure pore dynamics directly, but instead use exclusion to dyes of various sizes to determine pore size distribution [102]. The most direct measurement that is often made is the TMP [83], [103]. While the TMP may be extracted from either the SME or ASME, particularly when it is obtained self-consistently by considering the membrane conductivity as a function of pore density [104], which is a function of the applied PEF and resulting induced TMP, this still requires directly calculating the pore density using either the ASME or SME.

TABLE 1. Parameters used in the mathematical models.

Variable	Value
ε_o [99]	7.1×10^{-10} A · s · V^{-1}m^{-1}
ε_i [99]	7.1×10^{-10} A · s · V^{-1}m^{-1}
ε_m [99]	4.4×10^{-11} A · s · V^{-1}m^{-1}
λ_o [98]	1.2 S/m
λ_i [98]	0.3 S/m
λ_{m0} [99]	2.4×10^{-7} S/m
R [99]	15×10^{-6} m
d [99]	5×10^{-9} m
β	7
λ_p [98]	$\frac{\lambda_o - \lambda_i}{\ln(\lambda_o/\lambda_i)}$ S/m
K_1 [98]	$5 \times 10^{-9}\lambda_p$

Here, we derive a simple, computationally inexpensive electroporation model based strictly on electrical behavior. Rather than calculate pore dynamics directly, we incorporate a semi-empirical relationship between membrane conductivity and TMP [98] into an equation for the TMP based on solving Laplace's equations for a single-shell cell (i.e., a cell with no nucleus). From first principles, Kotnik et al. derived [99]

$$\Delta\Phi_m(t) = F(t)\,E(t)\,R\cos\theta, \tag{6}$$

where $E(t)$ is the applied electric field, R is the cell radius, θ is the polar angle, and $F(t)$ is a cell property dependent parameter defined by

$$\begin{aligned} F(t) = 3\Lambda_o\Big[&3dR^2\Lambda_i + \left(3d^2R - d^3\right)\left(\Lambda_m - \Lambda_i\right)\Big] \\ &\times\Big[2R^3\left(\Lambda_m + 2\Lambda_o\right)\left(\Lambda_m + \Lambda_i/2\right) \\ &-2\left(R - d\right)^3\left(\Lambda_o - \Lambda_m\right)\left(\Lambda_i - \Lambda_m\right)\Big]^{-1}, \end{aligned} \tag{7}$$

where d is the membrane thickness and the admittivity operators are given by

$$\Lambda_x = \lambda_x + \varepsilon_x\frac{d}{dt}, \tag{8}$$

where λ_x and ε_x are the conductivity and permittivity of the extracellular medium ($x = o$), cytoplasm ($x = i$), and membrane ($x = m$). While we use a simple single-shell model here for proof of principle, other more complicated models of TMP may ultimately be considered [105], [106], [107], [108]. Electroporation is incorporated into the membrane conductivity by the semi-empirical relationship [98]

$$\lambda_m(t) = \lambda_{m0} + K_1\left[\exp\left(\beta\left|\Delta\Phi_m(t)\right|\right) - 1\right], \tag{9}$$

where λ_{m0} is the initial membrane conductivity and β and K_1 are constants of the electroporation model. We consider $\lambda_m(t) = \lambda_{m0}$, which neglects dynamic changes due to electroporation, to benchmark to the results of Kotnik et al. [99] that consider a constant λ_m. Table 1 summarizes the parameters used in these calculations.

We next move the denominator of (7) to the left-hand side of (6), apply the derivatives to $E(t)$, $\lambda_m(t)$,and $\Delta\Phi_m(t)$, and combine terms to obtain an equation for $\Delta\Phi_m(t)$ incorporating electroporation effects with the left-hand side given by

$$\begin{aligned}
&\chi_1\Delta\Phi_m''(t)\\
&\quad+\chi_2\left[\left\{\lambda_{m0}+K_1\left[\exp\left(\beta\left|\Delta\Phi_m(t)\right|\right)-1\right]\right\}\Delta\Phi_m'(t)\right.\\
&\quad\left.+\beta K_1\exp\left(\beta\left|\Delta\Phi_m(t)\right|\right)\frac{\left(\Delta\Phi_m(t)\right)^2\left(\Delta\Phi_m'(t)\right)}{\left|\Delta\Phi_m(t)\right|}\right]\\
&\quad+\chi_3\Delta\Phi_m'(t)\\
&\quad+\chi_4\Delta\Phi_m(t)\left\{\lambda_{m0}+K_1\left[\exp\left(\beta\left|\Delta\Phi_m(t)\right|\right)-1\right]\right\}^2\\
&\quad+\chi_5\Delta\Phi_m(t)\left\{\lambda_{m0}+K_1\left[\exp\left(\beta\left|\Delta\Phi_m(t)\right|\right)-1\right]\right\}\\
&\quad+\chi_6\Delta\Phi_m(t),
\end{aligned} \tag{10}$$

and the right-hand side given by

$$\begin{aligned}
&\psi_1E''(t)\\
&\quad+\psi_2\left[\left\{\lambda_{m0}+K_1\left[\exp\left(\beta\left|\Delta\Phi_m(t)\right|\right)-1\right]\right\}E'(t)\right.\\
&\quad\left.+E(t)\,\beta K_1\exp\left(\beta\left|\Delta\Phi_m(t)\right|\right)\frac{\Delta\Phi_m(t)\left(\Delta\Phi_m'(t)\right)}{\left|\Delta\Phi_m(t)\right|}\right]\\
&\quad+\psi_3E'(t)\\
&\quad+\psi_4E(t)\left\{\lambda_{m0}+K_1\left[\exp\left(\beta\left|\Delta\Phi_m(t)\right|\right)-1\right]\right\}\\
&\quad+\psi_5E(t),
\end{aligned} \tag{11}$$

where the coefficients are given by

$$\begin{aligned}
\chi_1 &= 2d^3(\varepsilon_o-\varepsilon_m)(\varepsilon_i-\varepsilon_m)\\
&\quad+6Rd^2(\varepsilon_o-\varepsilon_m)(\varepsilon_m-\varepsilon_i)\\
&\quad+6dR^2(\varepsilon_o-\varepsilon_m)(\varepsilon_i-\varepsilon_m)+3\varepsilon_mR^3(2\varepsilon_o+\varepsilon_i)\\
\chi_2 &= 6d^2R(\varepsilon_o+\varepsilon_i-2\varepsilon_m)-2d^3(\varepsilon_o+\varepsilon_i-2\varepsilon_m)\\
&\quad-6dR^2(\varepsilon_o+\varepsilon_i-2\varepsilon_m)+3R^3(2\varepsilon_o+\varepsilon_i)\\
\chi_3 &= \left(2\varepsilon_i\lambda_0+2\varepsilon_o\lambda_i\right)(d-R)^3\\
&\quad+\left(2\varepsilon_i\lambda_o+4\varepsilon_m\lambda_o+2\varepsilon_o\lambda_i+\varepsilon_m\lambda_i\right)R^3\\
&\quad+\left(2\varepsilon_m\lambda_o+2\varepsilon_m\lambda_i\right)(R-d)^3\\
\chi_4 &= 2R^3-2(R-d)^3\\
\chi_5 &= \left(4\lambda_o+\lambda_i+2\lambda_o\lambda_i\right)R^3+\left(2\lambda_o+2\lambda_i-2\lambda_o\lambda_i\right)(R-d)^3\\
\chi_6 &= 2\lambda_o\lambda_iR^3-2\lambda_o\lambda_i(R-d)^3,
\end{aligned} \tag{12}$$

and

$$\begin{aligned}
\psi_1 &= (3dR\varepsilon_o\cos\theta)\left[d^2(\varepsilon_i-\varepsilon_m)\right.\\
&\quad\left.+3dR(\varepsilon_m-\varepsilon_i)+3R^2\varepsilon_i\right]\\
\psi_2 &= (3Rd\varepsilon_o\cos\theta)\left(3dR-d^2\right)\\
\psi_3 &= (3dR\cos\theta)\left[d^2\left(\varepsilon_i\lambda_o-\varepsilon_m\lambda_o+\varepsilon_o\lambda_i\right)\right.\\
&\quad\left.-3dR\left(\varepsilon_i\lambda_o-\varepsilon_m\lambda_o+\varepsilon_o\lambda_o\right)+3R^2\left(\varepsilon_i\lambda_o+\varepsilon_o\lambda_i\right)\right]\\
\psi_4 &= \left(3dR\lambda_o\cos\theta\right)\left(3dR-d^2\right)\\
\psi_5 &= (3dR\cos\theta)\,\lambda_o\lambda_i\left(d^2-3dR+3R^2\right).
\end{aligned} \tag{13}$$

Equations (11)-(13) represent the system of equations we will numerically solve for a given $E(t)$, since K_1 and β are assumed to be constants, leaving $\Delta\Phi_m(t)$ as the only unknown.

We consider the behavior during the duration of a square pulse of duration T {i.e., $E(t) = E_0[u_0(t) - u_T(t)]$, where $u_z(t) = 1$for $t > z$,} by modeling a unit step from $0 < t < T$ (i.e., neglecting the rise-and fall-times of a typical trapezoidal pulse). The TMP using this simple model is calculated by

$$\Delta\Phi_m(t) = \Delta\Phi_m(t)\,u_0(t) - x\times\Delta\Phi_m\left(t-T_{peak}\right)u_{T_{peak}}(t), \tag{14}$$

where x is the percent of the initial pulse being subtracted due to electroporation (i.e., x accounts for the suppression of the TMP due to pore formation) and T_{peak} is the time at which the peak TMP occurs (corresponding to electroporation). Without electroporation, $x = 1$. With electroporation, $x < 1$ (generally between 0.7 to 0.9) and is fit in the interpolation table. Again, the ASME models the applied electric field using a unit step function [i.e., $E(t) = E_0u_0(t)$], but only calculates through the pulse duration at $t = T$ to simulate the square pulse without explicitly accounting for the decay to $E(T) = 0$ at the end of the pulse.

While the ASME yields accurate results and is more computationally efficient than the full SME, our aim is to further reduce the computational expense required over a broad range of parameters of potential electrical stimulation. The long-term goal of the project is to assess the interactions of electrical stimulation on a multiscale level, including the (a) cell membrane, (b) whole cell, (c) surrounding tissue, (d) nerves (to assess action potential propagation and/or suppression), and (e) the full organism. The SME and ASME provide comprehensive analyses detailing pore dynamics and address (a) and (b). For (c)-(e), we aim to use tissue and/or animal models (such as a rat leg) from multiphysics software packages, such as Sim4Life (https://zmt.swiss/sim4life/) or COMSOL Multiphysics. The parametric analyses across various pulse parameters make the computational expense of the ASME (and SME) prohibitive.

For example, consider a 1 μs square pulse with an applied electric field amplitude of $E_0 = 6.75 \times 10^5$ V/m, a time step of $\Delta t = 0.5$ ns, and a total simulation time of 3 μs to compare simplified model (running in MATLAB) and the ASME (running in Python). With a standard personal laptop (e.g., 16 GB installed RAM and an Intel® Core™ i7-6500 processor) the simplified model outputs the solution in ∼10 s and the ASME completes in ∼30 s. While the time difference for these single pulses does not make the ASME prohibitive, the difference in computational expense greatly increases once we incorporate pulse trains or for more intense pulses that produce more pores. At that point, the burden of tracking the pore dynamics vastly increases the ASME computation time (e.g., a single 60 kV/cm, 60 ns pulse runs in ∼1 min and a train of five pulses runs in ∼19 min), while the simplified model's computation time will simply be multiplied by the number of pulses (e.g., if a single pulse runs in 10 s, a train of five pulses will run in 50 s). Thus, while the ASME is a robust model that can handle arbitrary waveforms and provide detailed pore dynamics, our simplified model empirically outperforms the ASME model—particularly for intense pulses and pulse trains that generate many pores. This makes this model a valuable computational tool. However, the results of the simplified model must still be benchmarked to those from the ASME to determine the various fitting parameters. High frequency electroporation is becoming increasingly important for improving transfection, making this process potentially valuable for predicting TMPs phenomenologically under pulse trains [109], [110], [111], further highlighting the need for computational tools that can effectively handle high numbers of pulses.

We accomplish this by considering three different time regimes during the stimulus: *Regime*1—from time $t = 0$ until the beginning of electroporation, which corresponds to the pore-induced arresting of the TMP increase at its peak [corresponding to the first term on the RHS of (14)]; *Regime*2—from the peak TMP until the end of the applied pulse at $t = T$ [corresponding to both terms on the RHS of (14)]; and *Regime 3*—from the end of the pulse until the end of the simulation time (corresponding to the exponential decay). We solve (10)-(13) numerically by fitting β for Regime 1, then subtract a portion of those results due to the enhanced membrane conductivity after the peak in accordance with (14) to fit x. In Regime 3, the TMP decays following PEF removal, so we assume exponential decay of the form

$$\Delta\Phi_m(t) = a\exp(-t/\tau), \tag{15}$$

where a and τ are fit from the results of the ASME. A parametric study between ASME and (10)-(15) for various applied field strengths and pulse durations yielded an interpolation table for a, τ, and x. For all cases considered in this study, $\beta = 7$.

Fig. 1 shows a, τ, and x for various pulse durations and electric fields. The "goodness" of the simplified model compared to the ASME model is quantified using

$$R^2 = 1 - \frac{\sum_{i=1}^{i=N}\left[\left(\Delta\Phi_{i,ASME} - \Delta\Phi_{i,Simplified}\right)^2\right]}{\sum_{i=1}^{i=N}\left[\left(\Delta\Phi_{i,ASME} - \bar{\Delta\Phi}_{avg}\right)^2\right]}, \tag{16}$$

where R^2 gives the coefficient of determination, $\Delta\Phi_{i,ASME}$ is the TMP of the ASME at each time step, $\Delta\Phi_{i,Simplified}$ is the TMP of the simplified model, and $\overline{\Delta\Phi}_{avg}$ is the time-averaged TMP of the ASME.

For RF fields and exponential pulses, given by $E(t) = E_0\cos(2\pi ft)$ and $E(t) = E_0\exp(-t/\tau_1)$, respectively, where f is frequency and τ_1 is the exponential time constant, we calculated the TMP below and above the electroporation threshold. Below the electroporation threshold, we simultaneously solved (10)-(13) with (9). However, at the beginning of electroporation, we substitute $\lambda_{m0} = \lambda_{m0,2}$ into (9) to account for the decrease in TMP due to the enhanced membrane conductivity due to pore formation. The two solutions are then assigned to the relevant time matrices in accordance with $\Delta\Phi_m(t) = \Delta\Phi_m(t)\,u_0(t) - \Delta\Phi_{m2}\left(t - T_{peak}\right)u_{T_{peak}}(t)$, where T_{peak} is the time at which $\Delta\Phi_m(t)$ reaches its peak before electroporation arrests TMP, which yields the full TMP solution. For $\Delta\Phi_{m2}$, $\lambda_m(t) = \lambda_{m0,2} + K_1\left[\exp(\beta\,|\Delta\Phi_m(t)|) - 1\right]$ the post-electroporation membrane conductivity is given by

$$\lambda_{m0,2} = \vartheta_1 E_0^2 + \vartheta_2 E_0 + \vartheta_3, \tag{17}$$

for an RF field, and

$$\lambda_{m0,2} = \vartheta_4 E_0^2 + \vartheta_5 E_0 + \vartheta_6, \tag{18}$$

for an exponential pulse, where the coefficients are defined as

$$\begin{aligned}
\vartheta_1 &= -9.9\times10^{-27}f^2 + 1.9\times10^{-20}f - 3.6\times10^{-15},\\
\vartheta_2 &= 6.3\times10^{-21}f^2 + 1.3\times10^{-14}f - 7.1\times10^{-9},\\
\vartheta_3 &= -5.2\times10^{-16}f^2 + 1.1\times10^{-9}f - 4.8\times10^{-4},\\
\vartheta_4 &= 2.36\times10^{-9}\tau_1 - 2.35\times10^{-15},\\
\vartheta_5 &= -1.14\times10^{-3}\tau_1 + 5.13\times10^{-9},\\
\vartheta_6 &= 1.79\times10^{2}\tau_1 - 5.78\times10^{-4},
\end{aligned} \tag{19}$$

where f is in Hz and τ_1 is in s. Furthermore, for a cosine field, $\beta = m_{cos}E_0 + b_{cos}$, where $m_{cos} = -7\times10^{-12}f + 6\times10^{-6}$ and $b_{cos} = 3\times10^{-6}f + 5$. For an exponential pulse, $\beta = 6.5$ below the electroporation threshold and $\beta = 8$ above the electroporation threshold. These semi-empirical fits came from parametric analyses and also recover the sub-electroporation behavior. Accounting for electroporation in this way allows us to incorporate its effects solely through the electrical properties (i.e., the membrane conductivity) without having to track pore dynamics which is especially helpful in high-field, short pulse duration cases where there are many small pores.

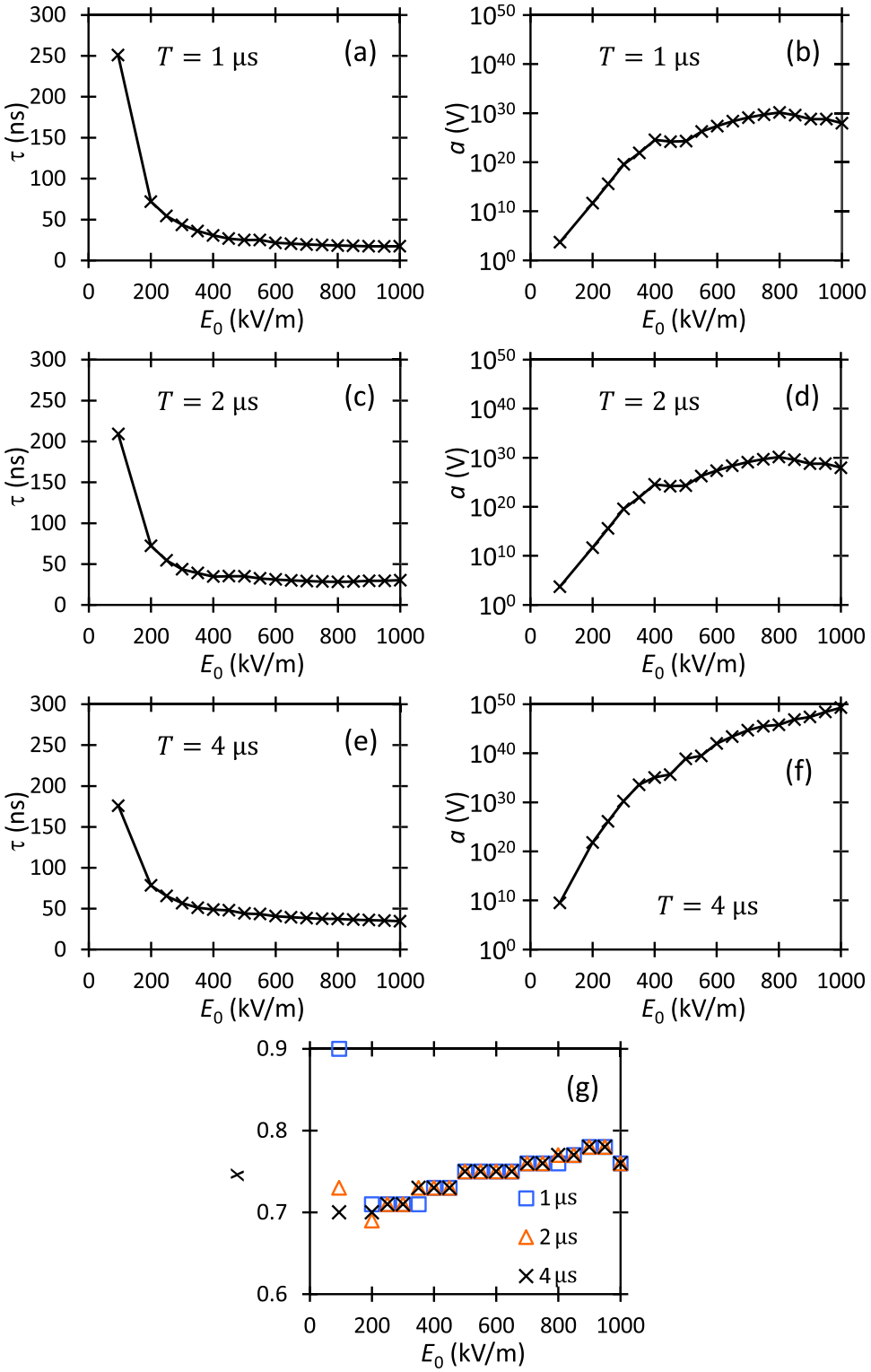

FIGURE 1. Fitting parameters as a function of applied electric field with τ shown in (a), (c), and (e), and a shown in (b), (d), and (f) for pulse durations of 1 μs (a-b), 2 μs (c-d) and 4 μs (e-f); x is shown in (g).

III. RESULTS

We next compare the results from the simplified electroporation model to the ASME. We fit the simplified model to the ASME to determine τ and a for an applied pulse as a function of E_0 for $T = 1$, 2, and 4 μs to create an interpolation table for assessing other PEFs. For each T considered, both τ and a

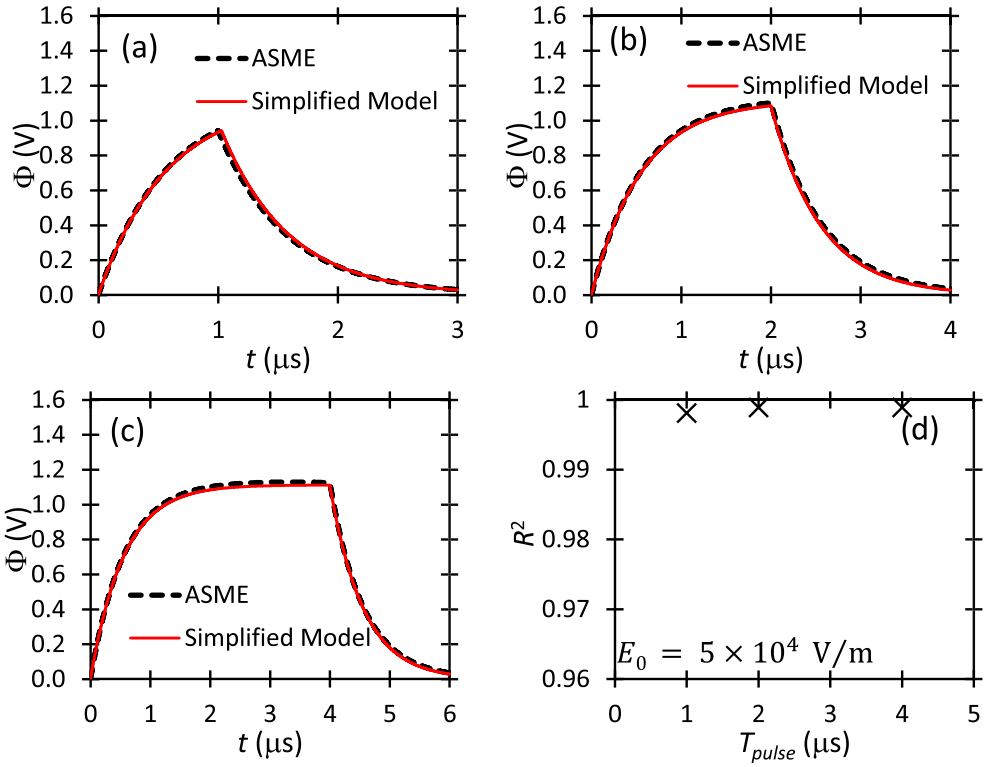

FIGURE 2. Transmembrane potential Φ as a function of time t in response to a unit step pulse for $E_0 = 5\times10^4$ V/m for pulse durations of (a) 1 μs, (b) 2 μs, and (c) 4 μs using the asymptotic Smoluchowski (ASME) equation and the simplified model, with the "goodness-of-fit" shown by R^2 in (d).

approach constants with increasing E_0 since pores eventually form; increasing E_0 further will not appreciably change TMP.

We then apply the interpolation table constructed from Fig. 1 to the simple model from (10)-(13) for an applied pulse to assess the quality of the fit to the ASME results. The comparison of the simplified model and ASME model is given by R^2, calculated using (16). Fig. 2 considers an applied PEF of $E_0 = 5\times10^4$ V/m, which is below the electroporation threshold and allows us to obtain an accurate fit without using the fitting parameters, since no membrane pore formation occurs. Fig. 3 applies $E_0 = 9.47 \times 10^4$ V/m to benchmark the simple model to previous ASME results [101] to validate both the ASME and simplified models. Figs. 4 and 5 consider $E_0 = 5\times10^5$ V/m and $E_0 = 1\times10^6$ V/m, respectively, which exceed the electroporation threshold. Figs. 2-5 consider pulse durations of (a) 1 μs, (b) 2 μs, and (c) 4 μs and report R^2 for each pulse duration.

Fig. 6 validates the simplified model by comparing the results using the simplified model with the fitting parameters to the ASME model for $E_0 = 6.75 \times 10^5$ V/m and $T = 1\mu$s. We determined $R^2 = 0.97$ between the ASME and simplified models, indicating excellent agreement between the two solutions when using the fitting parameter values from the interpolation table.

Fig. 7 demonstrates how we combine the solution responses for the exponential pulse (Fig. 7a) and the RF field (Fig. 7b). Figs. 8-10 compare the ASME to the simplified model for RF fields with frequencies of (8) 250 kHz, (9) 500 kHz, and (10) 1 MHz and electric field amplitudes of (a) 10 kV/m, (b) 100 kV/m, (c) 235 kV/m, and (d) 500 kV/m. The average agreement between the two models for these cases is $R^2 = 0.98$. These results indicate that the electric field required to induce electroporation increases with increasing frequency since the TMP for a given electric field amplitude decreases with increasing frequency. This behavior is consistent with prior calculations of TMP assuming constant membrane conductivity [99], which would correspond to sub-electroporation conditions.

Figs. 11 and 12 compare the ASME and simplified models for exponential pulses with time constants of $\tau_1 = 1\mu s$ and $\tau_1 = 2\mu$s, respectively, for electric field amplitudes of (a) $E_0 = 5 \times 10^4$ V/m, (b) $E_0 = 10^5$ V/m, (c) $E_0 = 3 \times 10^5$ V/m, and (d) $E_0 = 5 \times 10^5$ V/m. The average agreement between the two models for these cases is $R^2 = 0.96$.

While these results agree well with the ASME, both models assume minimal variation in the parameters in Table 1. Understanding the simplified model's sensitivity to these parameters is important. Ideally, we would perform a formal error propagation analysis as outlined in [112]; however, the lack of a closed form solution to the simplified model prevents us from directly applying this procedure. We can perform a parametric analysis by comparing the result

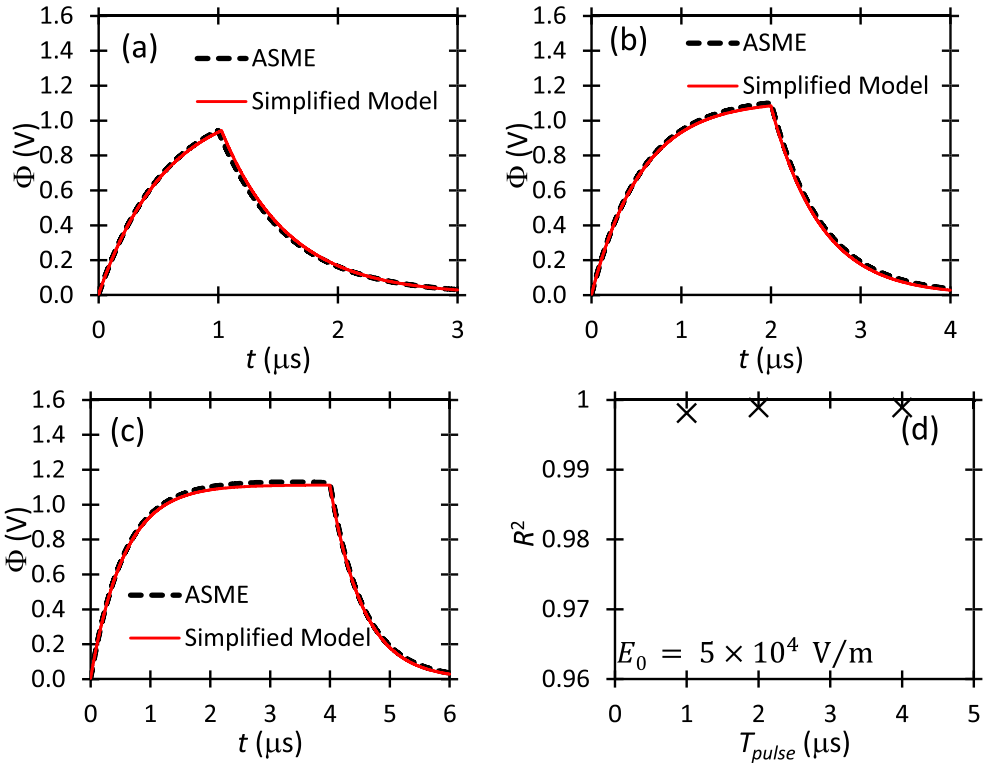

FIGURE 3. Transmembrane potential Φ as a function of time t in response to a unit step pulse for $E_0 = 9.47 \times 10^4$ V/m for pulse durations of (a) 1 μs, (b) 2 μs, and (c) 4 μs using the asymptotic Smoluchowski (ASME) equation and the simplified model, with the "goodness-of-fit" shown by R^2 in (d).

when we vary the cellular parameters from Table 1 to the original result obtained using Table 1. Considering the pulse parameters used for Fig. 6, we run the simplified model with each variable (i.e., ε_m, ε_0, ε_i, λ_0, λ_i, and λ_{m0}) having a different variation $\delta_{x_n} = 0.1, 0.3, 0.5, 0.7$, and 0.9 from its nominal value (e.g., $\delta_{x_n} x_n$ where $\delta_{x_n} = 1$ indicates no variation from the nominal value) and calculate R^2 between the resulting $\Delta\Phi$ and the nominal result (i.e., $\delta_{x_n} = 1$ for all parameters). Fig. 13 demonstrates that variation in λ_{m0} has no effect on $\Delta\Phi$, variation in ε_0 has minimal effect, and variation in λ_i and ε_m have the greatest effect.

We next expand the parametric analysis to examine how introducing variation in multiple parameters alters $\Delta\Phi$. Considering $\delta_{x_n} = 0.2, 0.4, 0.6, 0.8$, and 1 with $x_n = \varepsilon_m$, ε_i, λ_0, and λ_i gives a total of 625 simulations (and 625 R^2 values). Due to the difficulty in effectively reporting this large dataspace, we report the average R^2 over this range of data, R^2_{avg}, for the various conditions. For the square waveform, we obtain $R^2_{avg} = 0.72$. Repeating this analysis with the electrical parameters for the RF waveform from Fig. 9c and exponential waveform from Fig. 11c yields average $R^2_{avg} \sim 0.5$ and $\sim$0.6, respectively. Considering $\delta_{x_n} = 0.5, 0.6, 0.7, 0.8, 0.9$, and 1 gives the average R^2_{avg} of 0.9, 0.8, and 0.8 for the square, RF, and exponential waveforms, respectively. Thus, parameter variation is unlikely to dramatically influence calculations of TMP as long as $\delta_{x_n} > 0.5$ for each parameter. While performing a sensitivity analysis for the ASME would provide information that could improve the fidelity of the simplified model, the current model provides a reasonable first step for calculating TMP under various electrical waveforms.

IV. DISCUSSION

The main goal of this study was to develop and demonstrate a rapid, semi-empirical method for determining the effects of electrical waveforms on membrane permeabilization in spherical cells from strictly electrical arguments without directly calculating pore dynamics.

We first considered a pulse and determined the fitting parameters necessary to achieve excellent agreement between the simple and ASME models over a wide range of pulse durations. Fig. 2 shows that the TMP is characterized by a smooth increase, plateau, and subsequent decrease when below the electroporation threshold. Conversely, Fig. 3 demonstrates that just above the electroporation threshold, the TMP increases rapidly to its peak ($\sim$1.4 V) and then decreases sharply due to the onset of pore formation, before plateauing until the end of the pulse due to the presence of pores and decaying exponentially after the pulse ends. Figs. 3-6 demonstrate similar behavior, while also showing that the electroporation threshold and corresponding plateau occur more rapidly with increasing electric field. Of note,

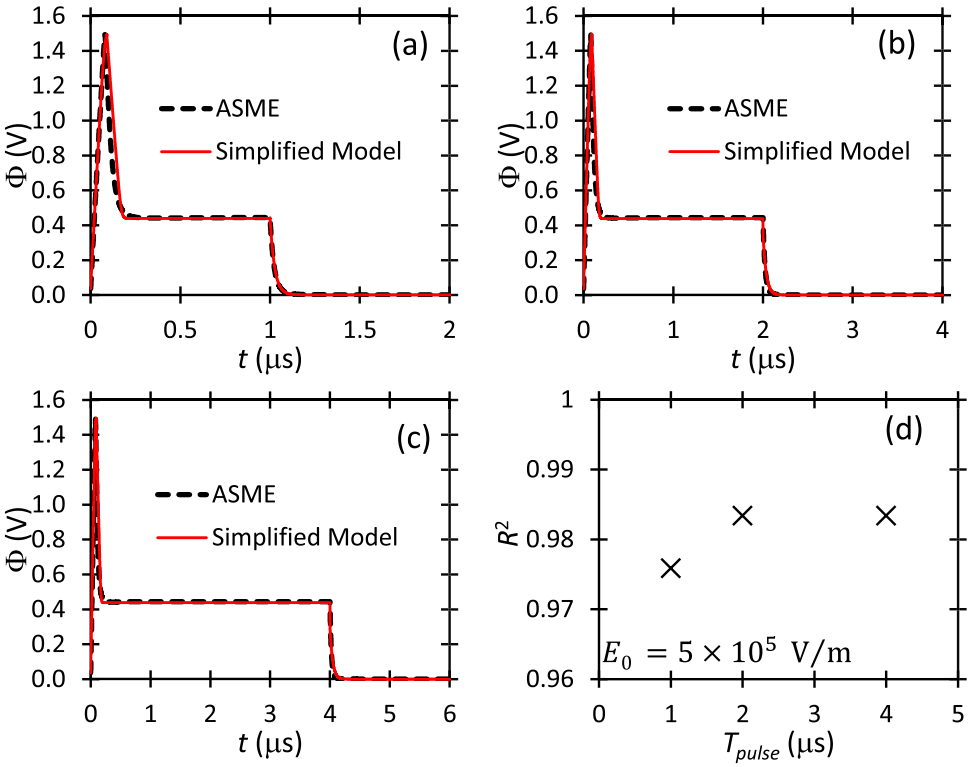

FIGURE 4. Transmembrane potential Φ as a function of time t in response to a unit step pulse for $E_0 = 5 \times 10^5$ V/m for pulse durations of (a) 1 μs, (b) 2 μs, and (c) 4 μs using the asymptotic Smoluchowski (ASME) equation and the simplified model, with the "goodness-of-fit" shown by R^2 in (d).

we used interpolated fitting parameters from the interpolation table to compare the simplified model to other ASME runs that were not used to obtain the table. Fig. 6 shows that the ASME and the simplified model agree well without having to directly fit the simplified model to the ASME. This indicates that the simplified model can recover the dynamics of ASME for a range of PEF parameters using the regimes for the fits and interpolation table developed here. This indicates the feasibility of using this simplified approach as a predictive tool for assessing multiscale and multiphysics phenomena rather than solely serving as a fit to the ASME.

Furthermore, this simplified model based strictly on electrical behavior without needing to directly assess pore dynamics also elucidates the behavior of TMP during electroporation. For instance, we directly incorporate the TMP-dependent membrane conductivity for the full pulse duration, showing the smooth initial TMP increase pre-electroporation, the rapid increase at the onset of electroporation, the sharp initial decrease due to rapid pore formation, the plateau of the TMP as pores are opening/closing, and the final exponential TMP decrease after the pulse is turned off.

In addition to traditional square-shaped PEFs, we also assessed RF fields and exponential pulses to demonstrate that the simplified approach works when the assumed temporal symmetry of the square pulse no longer exists. Figs. 8-10 show that a stronger electric field amplitude is necessary to induce electroporation at higher frequencies. For example, for $f = 250$ kHz, $E_0 = 100$ kV/m induces a slight degree of pore formation, as indicated through TMP behavior, while $E_0 = 235$ kV/m induces stronger pore formation. On the other hand, for $f = 1$ MHz, $E_0 = 235$ kV/m induces a slight degree of electroporation, while $E_0 = 500$ kV/m induces significant electroporation. Much as shorter duration PEFs fail to fully charge the membrane due to their high-frequency contents, narrowband RF fields of high-frequency will also fail to fully charge the membrane, resulting in a lower TMP than lower frequency fields [99]. Thus, a higher amplitude is necessary at higher frequencies to achieve the same TMP, and similar pore dynamics, as lower frequency fields. Figs. 11-12 demonstrate that the dynamics for exponential pulses with increasing time constant, which essentially makes the magnitude of the electric field higher for a longer duration, act similarly to increasing the duration for a square pulse.

These results demonstrate the effectiveness of assessing electroporation dynamics across a range of electrical waveforms by using strictly electrical behavior, specifically the TMP and assuming TMP-dependent membrane conductivity during PEF application. By not calculating the distribution of pore sizes, this approach reduces computational requirements across a range of electrical waveforms, particularly for high

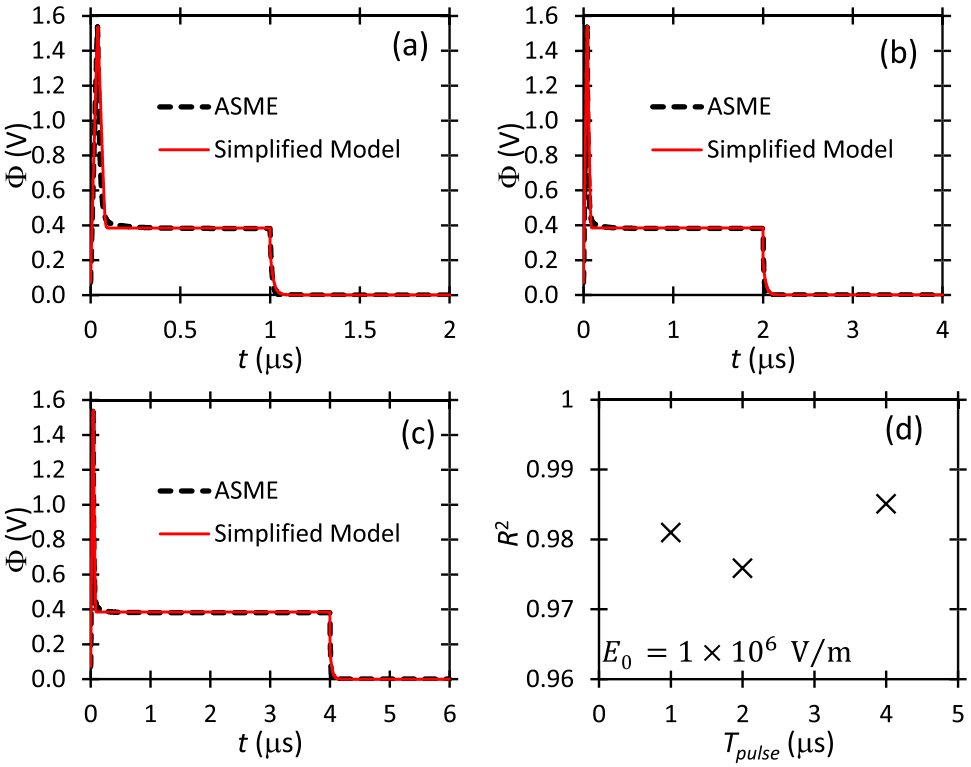

FIGURE 5. Transmembrane potential Φ as a function of time t in response to a unit step pulse for $E_0 = 1 \times 10^6$ V/m for pulse durations of (a) 1 μs, (b) 2 μs, and (c) 4 μs using the asymptotic Smoluchowski (ASME) equation and the simplified model, with the "goodness-of-fit" shown by R^2 in (d).

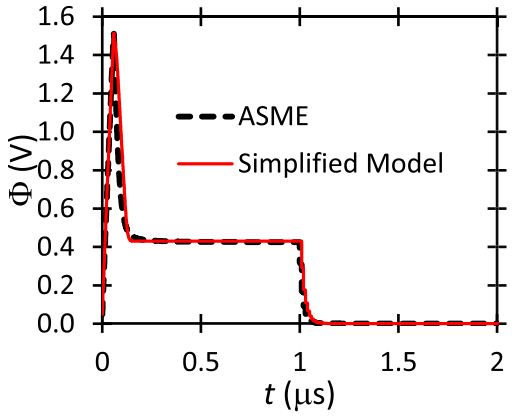

FIGURE 6. Transmembrane potential Φ as a function of time t in response to a unit step pulse for $E_0 = 6.75 \times 10^5$ V/m for a pulse duration of 1 μs using a, τ, β, and x values from the interpolation table. The R^2 value comparing the asymptotic Smoluchowski equation (ASME) and the simplified model is 0.97, indicating excellent agreement between the two.

intensity, short duration PEFs that generate a large density of small pores, which can be expensive even using the ASME rather than the full SME. While this method uses a semi-empirical approach to determine the fitting constant between the membrane conductivity and TMP, we have demonstrated that it yields excellent agreement with the ASME even for cases that we did not use to develop the fitting constants.

While some degree of fidelity in the model may be lost by not accurately calculating pore dynamics, this sort of approach provides value by only requiring electrical properties, which may be measured for cells of interest [113] and may also change during or after exposure [114]. Moreover, as Neu and Krassowska [86] pointed out when deriving the ASME, many of the parameters used in the SME are not readily known or measured, while the ASME and the simple electrical-based model we present here avoid this issue. Although the ASME and our simplified approach use fitted parameters, they tend to be based on phenomenological behavior that can be readily measured, such as the TMP. However, with the simplified approach, one does not gain insight into the spatial distribution of pores or ion/molecular transport; thus, the SME or ASME is necessary when those characteristics are of interest.

The simplified model provides a straightforward method to input desired pulse parameters and obtain the TMP as a function of time (i.e., a single array that is designed for initial multiphysics analyses). Conversely, the ASME outputs the TMP, pore density, pore size, pore location, and several other specific parameters at every time step *and* every polar angle (e.g., with 25 angular segments, as considered here, the TMP result alone consists of 25 of the arrays that the simplified model outputs). While these results are desirable for certain analyses, the amount of data quickly becomes unnecessarily cumbersome when the TMP at a specific

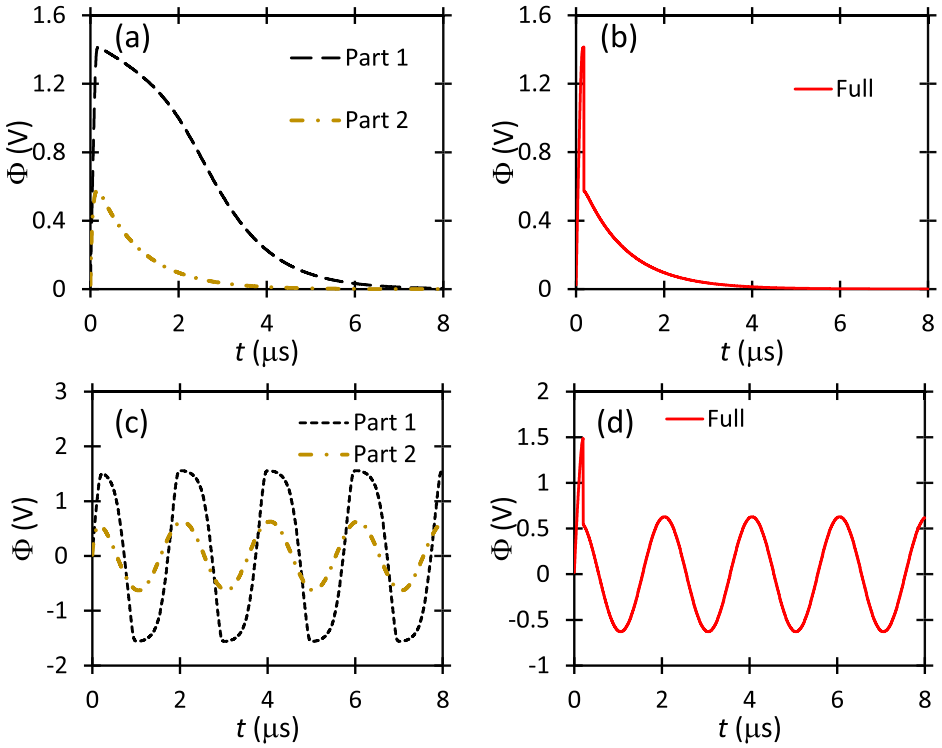

FIGURE 7. Demonstration of combination of solutions with λ_{m0} and $\lambda_{m0,2}$ for an (a) exponential waveform with $\tau = 1$ μs and $E_0 = 300$ kV/m and a (b) cosine waveform with f = 500 kHz and $E_0 = 235$ kV/m where Part 1 shows the numerical solution of (10)-(13) considering (9) as defined and Part 2 shows the numerical solution of (10)-(13) considering (9) with $\lambda_{m0} = \lambda_{m0,2}$.

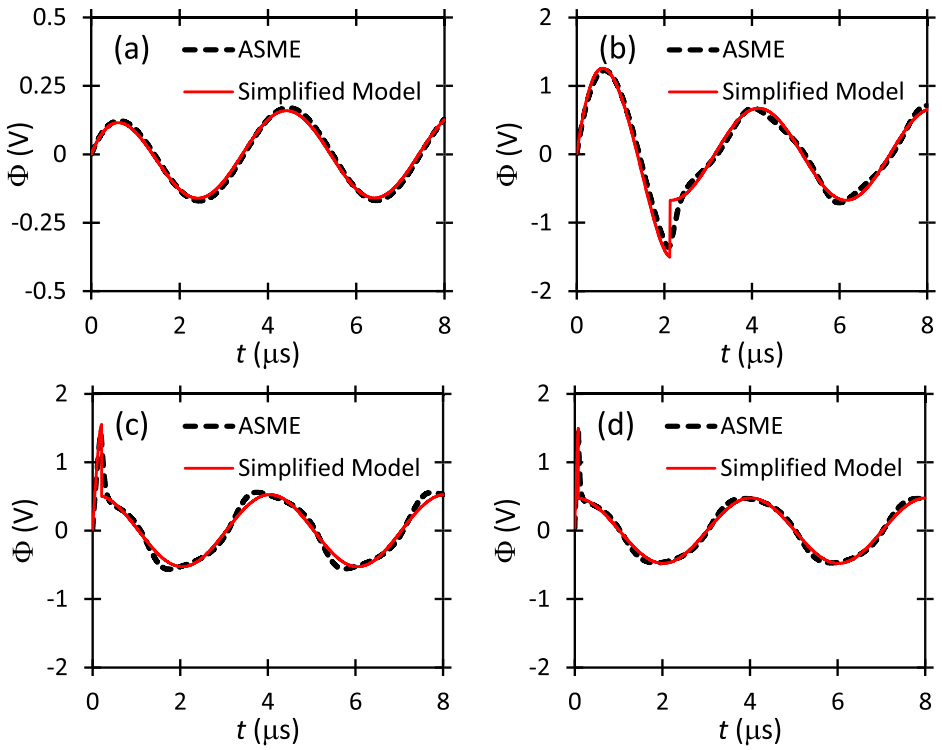

FIGURE 8. Transmembrane potential Φ as a function of time t in response to a cosine pulse for $f = 250$ kHz for applied electric field amplitudes of E_0 (a) 10 kV/m, (b) 100 kV/m, (c) 235 kV/m, and (d) 500 kV/m comparing the results of the asymptotic Smoluchowski (ASME) equation and the simplified theory.

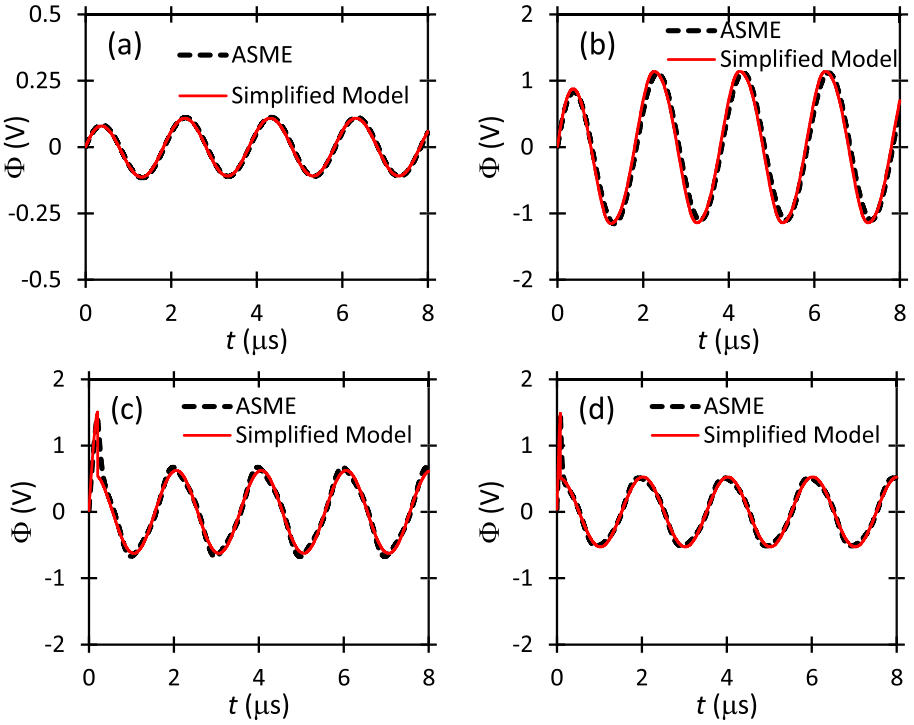

FIGURE 9. Transmembrane potential Φ as a function of time t in response to a cosine waveform for $f = 500$ kHz for applied electric field amplitudes of E_0 (a) 10 kV/m, (b) 100 kV/m, (c) 235 kV/m, and (d) 500 kV/m comparing the results of the asymptotic Smoluchowski (ASME) equation and the simplified theory.

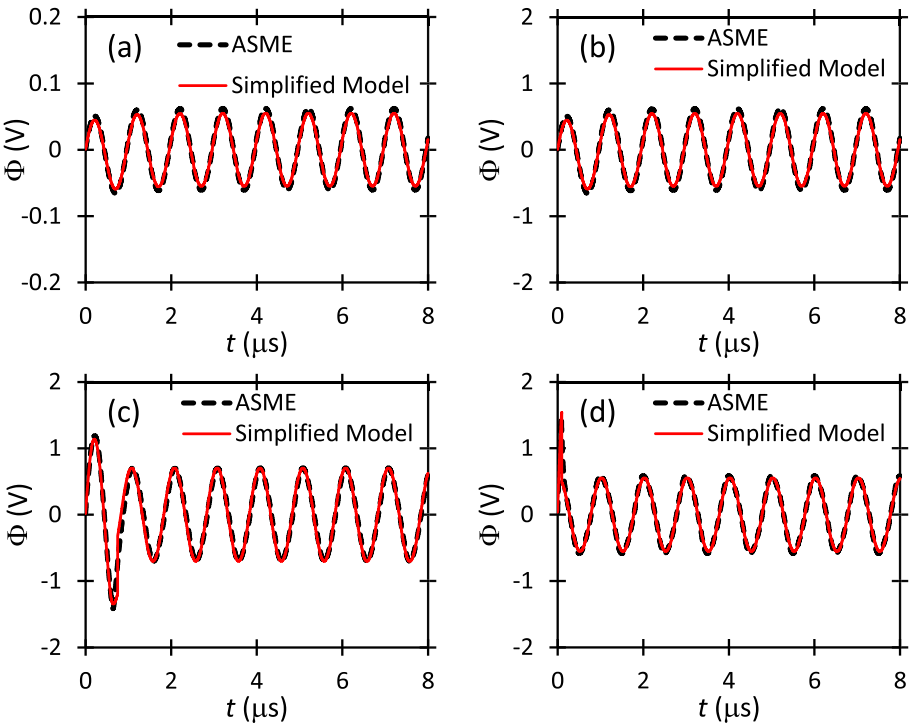

FIGURE 10. Transmembrane potential Φ as a function of time in response to a cosine waveform for $f = 1$ MHz for applied electric field amplitudes of E_0 (a) 10 kV/m, (b) 100 kV/m, (c) 235 kV/m, and (d) 500 kV/m comparing the results of the asymptotic Smoluchowski (ASME) equation and the simplified model.

angle is the only parameter of interest. Furthermore, the computational expense of the ASME for high-intensity pulses and pulse trains drastically increases, which would make the simplified model a more attractive option. Thus, the user can

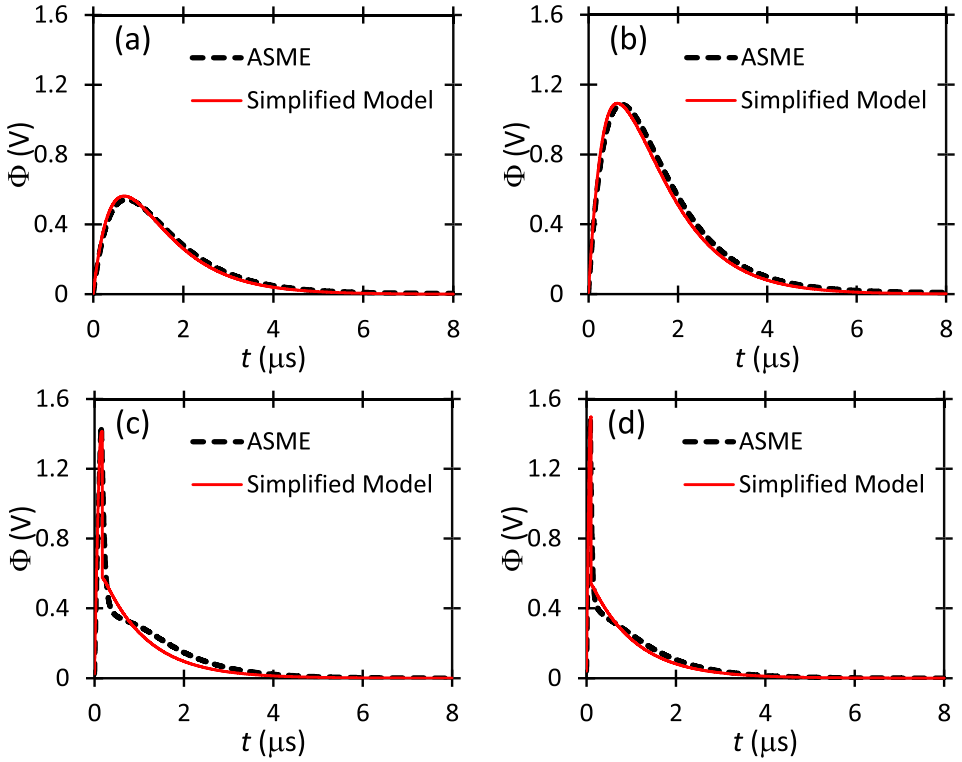

FIGURE 11. Transmembrane potential as a function of time in response to an exponential waveform for $\tau_1 = 1\mu$s for applied electric field amplitudes of E_0 (a) 50 kV/m, (b) 100 kV/m, (c) 300 kV/m, and (d) 500 kV/m comparing the results of the asymptotic Smoluchowski (ASME) equation and the simplified model.

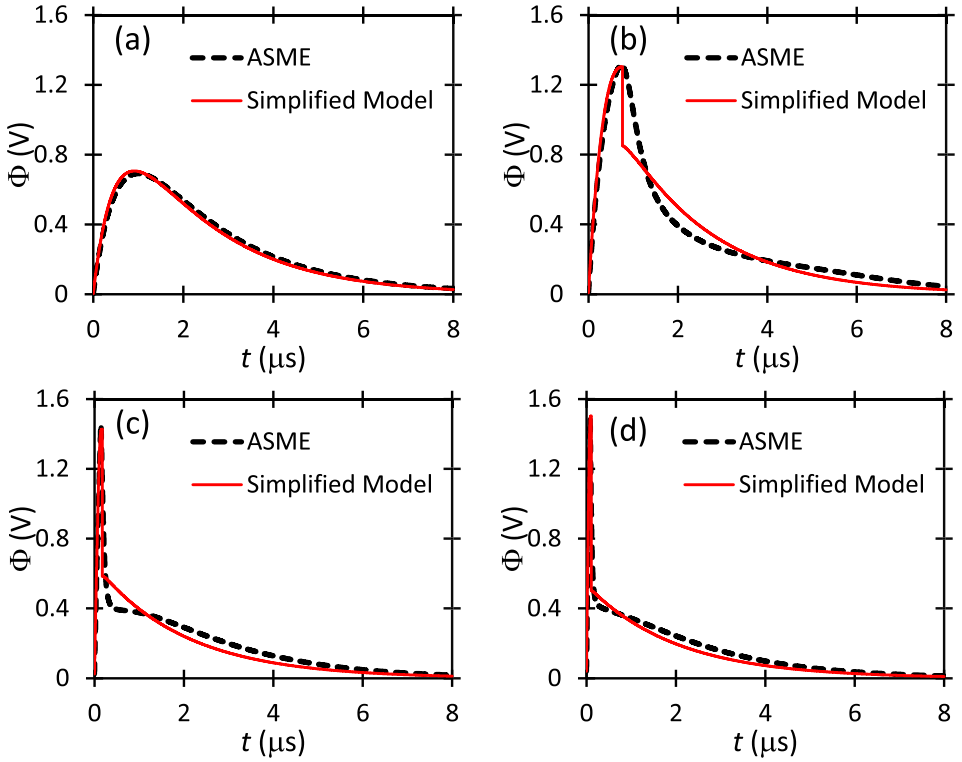

FIGURE 12. Transmembrane potential as a function of time in response to an exponential waveform for $\tau_1 = 2\mu$s for applied electric field amplitudes of E_0 (a) 50 kV/m, (b) 100 kV/m, (c) 300 kV/m, and (d) 500 kV/m using the asymptotic Smoluchowski (ASME) equation and the simplified model.

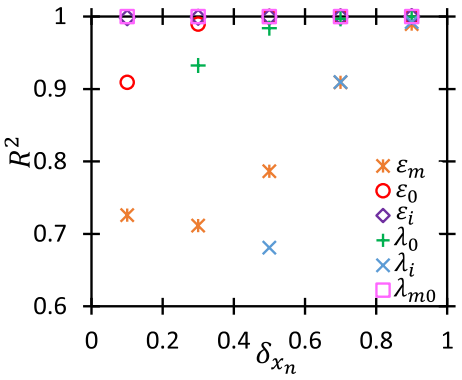

FIGURE 13. Assessment of R^2 comparing the simplified model with no variation in parameter to the simplified model with variation in a single parameter represented by the fraction δ_x, where $\delta \mathcal{D} 1$ indicates no variation (i.e.., $\delta_{x_n} x_n = x_n$, where $x_n = \varepsilon_m, \varepsilon_0, \varepsilon_i, \lambda_0, \lambda_i$, and λ_{m0}). Variation in λ_{m0} has no effect on $\Delta\Phi$, variation in ε_0 has minimal effect, and variations in λ_i and ε_m have the greatest effect.

choose the simplified model to rapidly estimate TMP for a multiscale or broad-sweeping parametric analysis or the ASME (or full SME) to provide information regarding pore dynamics or information regarding the angular distribution of the TMP. Ultimately, the ASME and simplified models both serve as options for assessing PEF-induced biological effects. The simplified model will serve as a foundational tool in future work assessing multiscale behavior in the presence of an electrical waveform.

Furthermore, future work will couple these results to Sim4Life to assess a full-scale model to provide insight into how these modified TMPs and additional shunt conductivities will influence the action potential initiation and propagation when starting from exposure to an electromagnetic waveform at the organism level. This analysis will aid in characterizing the multiscale effects of the PEFs and provide guidance for more in-depth simulation and experimental work to assist in biological, medical, and defense applications.

A. MODEL LIMITATIONS

While this study considers $\lambda_m(t)$, it assumes a constant ε_m. Extending this analysis to include a time-dependent membrane permeability will elucidate additional behavior and provide a more comprehensive prediction of TMP behavior with electroporation. Additionally, while we consider microsecond duration PEFs here for example cases, this approach could be applied to develop fitting functions for nano- or picosecond pulses and pulse trains. Furthermore, this additional analysis could aid in developing fitting functions for β, a, and τ for square pulses analogous to those derived for the RF and exponential pulses, which would mitigate the need for the interpolation table and improve the accuracy of the model.

V. CONCLUSION

We have developed a rapid method for calculating the TMP of cells permeabilized due to exposure to various electrical waveforms by applying a semi-empirical relationship between the membrane conductivity and the TMP without needing to directly calculate the pore dynamics. While the SME provides greater fidelity into pore dynamics, its computational expense makes it undesirable for rapidly assessing the pore formation as additional physical phenomena (such as temperature gradients and shock waves) are incorporated into multiphysics, multiscale models. Moreover, although the ASME alleviates some of this computational burden, it still requires tracking pore growth, which becomes computationally expensive when many pores are formed at shorter PEF durations (on the order of nanoseconds) and strong electric field intensities. The simplified model presented here demonstrates the feasibility of considering electropermeabilization strictly from an electrical perspective. This rapid model for membrane dynamics may ultimately be linked to tissue and organism level multiscale models for assessing the exposure to various electrical waveforms that may be relevant for occupational safety or therapies.

REFERENCES

[1] M. L. Yarmush, A. Golberg, G. SerŠa, T. Kotnik, and D. Miklavčič, "Electroporation-based technologies for medicine: Principles, applications, and challenges," *Annu. Rev. Biomed. Eng.*, vol. 16, no. 1, pp. 295–320, Jul. 2014.

[2] T. Kotnik, W. Frey, M. Sack, S. Haberl Meglič, M. Peterka, and D. Miklavčič, "Electroporation-based applications in biotechnology," *Trends Biotechnol.*, vol. 33, no. 8, pp. 480–488, Aug. 2015.

[3] R. P. Joshi, A. L. Garner, and R. Sundararajan, "Review of developments in bioelectrics as an application of pulsed power technology," *IEEE Trans. Plasma Sci.*, vol. 51, pp. 1682–1717, 2023.

[4] A. Sale and W. Hamilton, "Effects of high electric fields on microorganismsI. Killing of bacteria and yeasts," *Biochimica Biophysica Acta (BBA)-Gen. Subjects*, vol. 148, no. 3, pp. 781–788, Dec. 1967.

[5] A. J. H. Sale and W. A. Hamilton, "Effects of high electric fields on micro-organisms: III. Lysis of erythrocytes and protoplasts," *Biochim. Biophys. Acta, Biomembranes*, vol. 163, no. 1, pp. 37–43, Aug. 1968.

[6] A. L. Garner, "Pulsed electric field inactivation of microorganisms: From fundamental biophysics to synergistic treatments," *Appl. Microbiol. Biotechnol.*, vol. 103, no. 19, pp. 7917–7929, Oct. 2019.

[7] M. Pal, "Pulsed electric field processing: An emerging technology for food preservation," *J. Experim. Food Chem.*, vol. 3, no. 2, 2017, Art. no. 2.

[8] C. Vaquero, I. Loira, J. Raso, I. Álvarez, C. Delso, and A. Morata, "Pulsed electric fields to improve the use of non-saccharomyces starters in red wines," *Foods*, vol. 10, no. 7, p. 1472, Jun. 2021.

[9] S. van Wyk, F. V. M. Silva, and M. M. Farid, "Pulsed electric field treatment of red wine: Inactivation of brettanomyces and potential hazard caused by metal ion dissolution," *Innov. Food Sci. Emerg. Technol.*, vol. 52, pp. 57–65, Mar. 2019.

[10] G. Rios-Corripio, M. M.-D. la Peña, J. Welti-Chanes, and J. Á. Guerrero-Beltrán, "Pulsed electric field processing of a pomegranate (*Punica granatum L.*) fermented beverage," *Innov. Food Sci. Emerg. Technol.*, vol. 79, Jul. 2022, Art. no. 103045.

[11] S. Yildiz, P. R. Pokhrel, S. Unluturk, and G. V. Barbosa-Cánovas, "Shelf life extension of strawberry juice by equivalent ultrasound, high pressure, and pulsed electric fields processes," *Food Res. Int.*, vol. 140, Feb. 2021, Art. no. 110040.

[12] A. Šalaševičius, D. Uždavinytė, M. Visockis, P. Ruzgys, and S. Šatkauskas, "Effect of pulsed electric field (PEF) on bacterial viability and whey protein in the processing of raw milk," *Appl. Sci.*, vol. 11, no. 23, p. 11281, Nov. 2021.

[13] B. Preeti, M. R. Ravindra, B. S. Nath, and D. G. Panditrao, "Impact of pulsed electric field treated milk on quality of *paneer* and *khoa*," *Food Sci. Technol. Int.*, vol. 29, no. 6, pp. 598–609, Sep. 2023.

[14] V. Novickij, R. Stanevičienė, A. Grainys, J. Lukša, K. Badokas, T. Krivorotova, J. Sereikaitė, J. Novickij, and E. Servienė, "Electroporation-assisted inactivation of *Escherichia coli* using nisin-loaded pectin nanoparticles," *Innov. Food Sci. Emerg. Technol.*, vol. 38, pp. 98–104, Dec. 2016.

[15] V. Novickij, R. Stanevičienė, G. Staigvila, R. Gruškienė, J. Sereikaitė, I. Girkontaitė, J. Novickij, and E. Servienė, "Effects of pulsed electric fields and mild thermal treatment on antimicrobial efficacy of nisin-loaded pectin nanoparticles for food preservation," *LWT*, vol. 120, Feb. 2020, Art. no. 108915.

[16] Z. Yan, L. Yin, C. Hao, K. Liu, and J. Qiu, "Synergistic effect of pulsed electric fields and temperature on the inactivation of microorganisms," *AMB Exp.*, vol. 11, no. 1, Dec. 2021, Art. no. 47.

[17] C. Delso, A. Berzosa, J. Sanz, I. Álvarez, and J. Raso, "Pulsed electric field processing as an alternative to sulfites (SO_2) for controlling *Saccharomyces cerevisiae* involved in the fermentation of *Chardonnay* white wine," *Food Res. Int.*, vol. 165, Mar. 2023, Art. no. 112525.

[18] C. Delso, A. Berzosa, J. Sanz, I. Álvarez, and J. Raso, "Microbial decontamination of red wine by pulsed electric fields (PEF) after alcoholic and malolactic fermentation: Effect on *Saccharomyces cerevisiae*, *Oenococcus oeni*, and oenological parameters during storage," *Foods*, vol. 12, no. 2, Jan. 2023, Art. no. 278.

[19] U. Probst, I. Fuhrmann, L. Beyer, and P. Wiggermann, "Electrochemotherapy as a new modality in interventional oncology: A review," *Technol. Cancer Res. Treatment*, vol. 17, Jan. 2018, Art. no. 153303381878532.

[20] L. Lambricht, A. Lopes, S. Kos, G. Sersa, V. Préat, and G. Vandermeulen, "Clinical potential of electroporation for gene therapy and DNA vaccine delivery," *Expert Opinion Drug Del.*, vol. 13, no. 2, pp. 295–310, Feb. 2016.

[21] S. K. Frandsen, M. Vissing, and J. Gehl, "A comprehensive review of calcium electroporation—A novel cancer treatment modality," *Cancers*, vol. 12, no. 2, Jan. 2020, Art. no. 290.

[22] B. Geboers, H. J. Scheffer, P. M. Graybill, A. H. Ruarus, S. Nieuwenhuizen, R. S. Puijk, P. M. van den Tol, R. V. Davalos, B. Rubinsky, T. D. de Gruijl, D. Miklavčič, and M. R. Meijerink, "High-voltage electrical pulses in oncology: Irreversible electroporation, electrochemotherapy, gene electrotransfer, electrofusion, and electroimmunotherapy," *Radiology*, vol. 295, no. 2, pp. 254–272, May 2020.

[23] R. Nuccitelli, "Application of pulsed electric fields to cancer therapy," *Bioelectricity*, vol. 1, no. 1, pp. 30–34, Mar. 2019.

[24] M. P. Rols, Y. Tamzali, and J. Teissié, "Electrochemotherapy of horses. A preliminary clinical report," *Bioelectrochemistry*, vol. 55, nos. 1–2, pp. 101–105, Jan. 2002.

[25] M. Cemazar, G. Sersa, and M. Auersperg, "Antitumor effectiveness of bolus versus split dose vinblastine treatment in EAT tumors in mice," *Anticancer Res.*, vol. 17, pp. 4553–4556, Jan. 1997.

[26] E. P. Spugnini and A. Baldi, "Electrochemotherapy in veterinary oncology," *Veterinary Clinics North America: Small Animal Pract.*, vol. 49, no. 5, pp. 967–979, Sep. 2019.

[27] G. Sersa, D. Miklavcic, M. Cemazar, Z. Rudolf, G. Pucihar, and M. Snoj, "Electrochemotherapy in treatment of tumours," *Eur. J. Surgical Oncol. (EJSO)*, vol. 34, no. 2, pp. 232–240, Feb. 2008.

[28] I. Tsoneva, S. Semkova, R. Bakalova, Z. Zhelev, P. Nuss, G. Staneva, and B. Nikolova, "Electroporation, electrochemotherapy and electro-assisted drug delivery in cancer. A state-of-the-art review," *Biophys. Chem.*, vol. 286, Jul. 2022, Art. no. 106819.

[29] A. L. Garner, A. L. Frelinger, A. J. Gerrits, T. Gremmel, E. E. Forde, S. L. Carmichael, A. D. Michelson, and V. B. Neculaes, "Using extracellular calcium concentration and electric pulse conditions to tune platelet-rich plasma growth factor release and clotting," *Med. Hypotheses*, vol. 125, pp. 100–105, Apr. 2019.

[30] B. Neculaes, A. L. Garner, S. Klopman, and E. A. Longman, "Dependence of electric pulse mediated growth factor release on the platelet rich plasma separation method," *Appl. Sci.*, vol. 12, no. 10, May 2022, Art. no. 4965.

[31] J. Zhang, P. F. Blackmore, B. Y. Hargrave, S. Xiao, S. J. Beebe, and K. H. Schoenbach, "Nanosecond pulse electric field (nanopulse): A novel non-ligand agonist for platelet activation," *Arch. Biochem. Biophys.*, vol. 471, no. 2, pp. 240–248, Mar. 2008.

[32] M. Wu, A. E. Rubin, T. Dai, R. Schloss, O. B. Usta, A. Golberg, and M. Yarmush, "High-voltage, pulsed electric fields eliminate *Pseudomonas aeruginosa* stable infection in a mouse burn model," *Adv. Wound Care*, vol. 10, no. 9, pp. 477–489, Sep. 2021.

[33] A. Vadlamani, D. A. Detwiler, A. Dhanabal, and A. L. Garner, "Synergistic bacterial inactivation by combining antibiotics with nanosecond electric pulses," *Appl. Microbiol. Biotechnol.*, vol. 102, no. 17, pp. 7589–7596, Sep. 2018.

[34] V. Novickij, J. Švedienė, A. Paškevičius, S. Markovskaja, I. Girkontaitė, A. Zinkevičienė, E. Lastauskienė, and J. Novickij, "Pulsed electric field-assisted sensitization of multidrug-resistant *Candida albicans* to antifungal drugs," *Future Microbiol.*, vol. 13, no. 5, pp. 535–546, Apr. 2018.

[35] A. R. Khan, S. Khan, M. A. Sheikh, S. Khuder, B. Grubb, and G. V. Moukarbel, "Catheter ablation and antiarrhythmic drug therapy as first- or second-line therapy in the management of atrial fibrillation: Systematic review and meta-analysis," *Circulat., Arrhythmia Electrophysiol.*, vol. 7, no. 5, pp. 853–860, Oct. 2014.

[36] F. Xie, F. Varghese, A. G. Pakhomov, I. Semenov, S. Xiao, J. Philpott, and C. Zemlin, "Ablation of myocardial tissue with nanosecond pulsed electric fields," *PLoS ONE*, vol. 10, no. 12, Dec. 2015, Art. no. e0144833.

[37] F. Varghese, J. M. Philpott, J. U. Neuber, B. Hargrave, and C. W. Zemlin, "Surgical ablation of cardiac tissue with nanosecond pulsed electric fields in swine," *Cardiovascular Eng. Technol.*, vol. 14, no. 1, pp. 52–59, Feb. 2023.

[38] M. T. Stewart, D. E. Haines, A. Verma, N. Kirchhof, N. Barka, E. Grassl, and B. Howard, "Intracardiac pulsed field ablation: Proof of feasibility in a chronic porcine model," *Heart Rhythm*, vol. 16, no. 5, pp. 754–764, May 2019.

[39] R. Bocker and E. K. Silva, "Pulsed electric field assisted extraction of natural food pigments and colorings from plant matrices," *Food Chem., X*, vol. 15, Oct. 2022, Art. no. 100398.

[40] M. M. A. N. Ranjha, R. Kanwal, B. Shafique, R. N. Arshad, S. Irfan, M. Kieliszek, P. Kowalczewski, M. Irfan, M. Z. Khalid, U. Roobab, and R. M. Aadil, "A critical review on pulsed electric field: A novel technology for the extraction of phytoconstituents," *Molecules*, vol. 26, no. 16, Aug. 2021, Art. no. 4893.

[41] J. Xi, Z. Li, and Y. Fan, "Recent advances in continuous extraction of bioactive ingredients from food-processing wastes by pulsed electric fields," *Crit. Rev. Food Sci. Nutrition*, vol. 61, no. 10, pp. 1738–1750, May 2021.

[42] Z. Chen and W. G. Lee, "Electroporation for microalgal biofuels: A review," *Sustain. Energy Fuels*, vol. 3, no. 11, pp. 2954–2967, 2019.

[43] P. Geada, R. Rodrigues, L. Loureiro, R. Pereira, B. Fernandes, J. A. Teixeira, V. Vasconcelos, and A. A. Vicente, "Electrotechnologies applied to microalgal biotechnology—Applications, techniques and future trends," *Renew. Sustain. Energy Rev.*, vol. 94, pp. 656–668, Oct. 2018.

[44] J. Martínez, C. Delso, I. Álvarez, and J. Raso, "Pulsed electric field-assisted extraction of valuable compounds from microorganisms," *Comprehensive Rev. Food Sci. Food Saf.*, vol. 19, pp. 539–552, Mar. 2020.

[45] C. H. Geissler, M. L. Mulligan, Z. E. Zmola, S. Ray, J. A. Morgan, and A. L. Garner, "Electric pulse pretreatment for enhanced lipid recovery from chlorella protothecoides," *BioEnergy Res.*, vol. 13, no. 2, pp. 499–506, Jun. 2020.

[46] M. Goettel, C. Eing, C. Gusbeth, R. Straessner, and W. Frey, "Pulsed electric field assisted extraction of intracellular valuables from microalgae," *Algal Res.*, vol. 2, no. 4, pp. 401–408, Oct. 2013.

[47] W. Frey, C. Gusbeth, and T. Schwartz, "Inactivation of *Pseudomonas putida* by pulsed electric field treatment: A study on the correlation of treatment parameters and inactivation efficiency in the short-pulse range," *J. Membrane Biol.*, vol. 246, no. 10, pp. 769–781, Oct. 2013.

[48] D. P. Jaeschke, G. D. Mercali, L. D. F. Marczak, G. Müller, W. Frey, and C. Gusbeth, "Extraction of valuable compounds from *Arthrospira platensis* using pulsed electric field treatment," *Bioresource Technol.*, vol. 283, pp. 207–212, Jul. 2019.

[49] S. Akaberi, D. Krust, G. Müller, W. Frey, and C. Gusbeth, "Impact of incubation conditions on protein and C-phycocyanin recovery from *Arthrospira platensis* post- pulsed electric field treatment," *Bioresource Technol.*, vol. 306, Jun. 2020, Art. no. 123099.

[50] I. Papachristou, S. Akaberi, A. Silve, E. Navarro-López, R. Wüstner, K. Leber, N. Nazarova, G. Müller, and W. Frey, "Analysis of the lipid extraction performance in a cascade process for *Scenedesmus almeriensis* biorefinery," *Biotechnol. Biofuels*, vol. 14, no. 1, Dec. 2021, Art. no. 20.

[51] C. Delso, A. Silve, R. Wüstner, N. Nazarova, I. Álvarez, J. Raso, and W. Frey, "Post-incubation pH impacts the lipid extraction assisted by pulsed electric fields from wet biomass of *Auxenochlorella protothecoides*," *ACS Sustain. Chem. Eng.*, vol. 10, no. 37, pp. 12448–12456, Sep. 2022.

[52] M. D. A. Zbinden, B. S. M. Sturm, R. D. Nord, W. J. Carey, D. Moore, H. Shinogle, and S. M. Stagg-Williams, "Pulsed electric field (PEF) as an intensification pretreatment for greener solvent lipid extraction from microalgae," *Biotechnol. Bioeng.*, vol. 110, no. 6, pp. 1605–1615, Jun. 2013.

[53] L. Buchmann, I. Brändle, I. Haberkorn, M. Hiestand, and A. Mathys, "Pulsed electric field based cyclic protein extraction of microalgae towards closed-loop biorefinery concepts," *Bioresource Technol.*, vol. 291, Nov. 2019, Art. no. 121870.

[54] S. Bensalem, D. Pareau, B. Cinquin, O. Français, B. Le Pioufle, and F. Lopes, "Impact of pulsed electric fields and mechanical compressions on the permeability and structure of *Chlamydomonas reinhardtii* cells," *Sci. Rep.*, vol. 10, no. 1, Feb. 2020, Art. no. 2668.

[55] H. Gateau, V. Blanckaert, B. Veidl, O. Burlet-Schiltz, C. Pichereaux, A. Gargaros, J. Marchand, and B. Schoefs, "Application of pulsed electric fields for the biocompatible extraction of proteins from the microalga *Haematococcus pluvialis*," *Bioelectrochemistry*, vol. 137, Feb. 2021, Art. no. 107588.

[56] O. Parniakov, F. J. Barba, N. Grimi, L. Marchal, S. Jubeau, N. Lebovka, and E. Vorobiev, "Pulsed electric field and pH assisted selective extraction of intracellular components from microalgae *Nannochloropsis*," *Algal Res.*, vol. 8, pp. 128–134, Mar. 2015.

[57] K. N. Aycock and R. V. Davalos, "Irreversible electroporation: Background, theory, and review of recent developments in clinical oncology," *Bioelectricity*, vol. 1, no. 4, pp. 214–234, Dec. 2019.

[58] C. Jiang, R. V. Davalos, and J. C. Bischof, "A review of basic to clinical studies of irreversible electroporation therapy," *IEEE Trans. Biomed. Eng.*, vol. 62, no. 1, pp. 4–20, Jan. 2015.

[59] R. C. G. Martin, K. McFarland, S. Ellis, and V. Velanovich, "Irreversible electroporation in locally advanced pancreatic cancer: Potential improved overall survival," *Ann. Surgical Oncol.*, vol. 20, no. S3, pp. 443–449, Dec. 2013.

[60] R. C. G. Martin, A. N. Durham, M. G. Besselink, D. Iannitti, M. J. Weiss, C. L. Wolfgang, and K.-W. Huang, "Irreversible electroporation in locally advanced pancreatic cancer: A call for standardization of energy delivery," *J. Surgical Oncol.*, vol. 114, no. 7, pp. 865–871, Dec. 2016.

[61] A. H. Ruarus, L. G. P. H. Vroomen, B. Geboers, E. van Veldhuisen, R. S. Puijk, S. Nieuwenhuizen, M. G. Besselink, B. M. Zonderhuis, G. Kazemier, T. D. de Gruijl, K. P. van Lienden, J. J. J. de Vries, H. J. Scheffer, and M. R. Meijerink, "Percutaneous irreversible electroporation in locally advanced and recurrent pancreatic cancer (PANFIRE-2): A multicenter, prospective, single-arm, phase II study," *Radiology*, vol. 294, no. 1, pp. 212–220, Jan. 2020.

[62] L. Miller, J. Leor, and B. Rubinsky, "Cancer cells ablation with irreversible electroporation," *Technol. Cancer Res. Treatment*, vol. 4, no. 6, pp. 699–705, Dec. 2005.

[63] B. Al-Sakere, F. André, C. Bernat, E. Connault, P. Opolon, R. V. Davalos, B. Rubinsky, and L. M. Mir, "Tumor ablation with irreversible electroporation," *PLoS ONE*, vol. 2, no. 11, Nov. 2007, Art. no. e1135.

[64] M. R. Bower, Y. Li, Q. Liu, and R. C. Martin, "Irreversible electroporation of the pancreas: Definitive local therapy without systemic effects," *J. Surgical Res.*, vol. 158, no. 2, pp. 394–395, Feb. 2010.

[65] R. V. Davalos, L. M. Mir, and B. Rubinsky, "Tissue ablation with irreversible electroporation," *Ann. Biomed. Eng.*, vol. 33, no. 2, pp. 223–231, 2005.

[66] R. Nuccitelli, U. Pliquett, X. Chen, W. Ford, R. J. Swanson, S. J. Beebe, J. F. Kolb, and K. H. Schoenbach, "Nanosecond pulsed electric fields cause melanomas to self-destruct," *Biochem. Biophys. Res. Commun.*, vol. 343, no. 2, pp. 351–360, May 2006.

[67] S. J. Beebe, P. M. Fox, L. J. Rec, K. Somers, R. H. Stark, and K. H. Schoenbach, "Nanosecond pulsed electric field (nsPEF) effects on cells and tissues: Apoptosis induction and tumor growth inhibition," *IEEE Trans. Plasma Sci.*, vol. 30, no. 1, pp. 286–292, Feb. 2002.

[68] S. J. Beebe, P. M. Fox, L. J. Rec, L. K. Willis, and K. H. Schoenbach, "Nanosecond, high-intensity pulsed electric fields induce apoptosis in human cells," *FASEB J.*, vol. 17, no. 11, pp. 1–23, Aug. 2003.

[69] R. P. Joshi, A. Mishra, Q. Hu, K. H. Schoenbach, and A. Pakhomov, "Self-consistent analyses for potential conduction block in nerves by an ultrashort high-intensity electric pulse," *Phys. Rev. E, Stat. Phys. Plasmas Fluids Relat. Interdiscip. Top.*, vol. 75, no. 6, Jun. 2007, Art. no. 061906.

[70] S. W. Kuffler and R. W. Gerard, "The small-nerve motor system to skeletal muscle," *J. Neurophysiol.*, vol. 10, no. 6, pp. 383–394, Nov. 1947.

[71] J. G. Whitwam and C. Kidd, "The use of direct current to cause selective block of large fibres in peripheral nerves," *Brit. J. Anaesthesia*, vol. 47, no. 11, pp. 1123–1132, Nov. 1975.

[72] K. Schoenbach, B. Hargrave, R. Joshi, J. Kolb, R. Nuccitelli, C. Osgood, A. Pakhomov, M. Stacey, R. Swanson, J. White, S. Xiao, J. Zhang, S. Beebe, P. Blackmore, and E. Buescher, "Bioelectric effects of intense nanosecond pulses," *IEEE Trans. Dielectr. Electr. Insul.*, vol. 14, no. 5, pp. 1088–1109, Oct. 2007.

[73] S.-J. Tsai, H. L. Lew, E. Date, and L.-I. Bih, "Treatment of detrusor-sphincter dyssynergia by pudendal nerve block in patients with spinal cord injury," *Arch. Phys. Med. Rehabil.*, vol. 83, no. 5, pp. 714–717, May 2002.

[74] J. C. Weaver and Y. A. Chizmadzhev, "Theory of electroporation: A review," *Bioelectrochem. Bioenergetics*, vol. 41, no. 2, pp. 135–160, Dec. 1996.

[75] R. P. Joshi and K. H. Schoenbach, "Mechanism for membrane electroporation irreversibility under high-intensity, ultrashort electrical pulse conditions," *Phys. Rev. E, Stat. Phys. Plasmas Fluids Relat. Interdiscip. Top.*, vol. 66, no. 5, Nov. 2002, Art. no. 052901.

[76] K. H. Schoenbach, R. P. Joshi, J. F. Kolb, N. Chen, M. Stacey, P. F. Blackmore, E. S. Buescher, and S. J. Beebe, "Ultrashort electrical pulses open a new gateway into biological cells," *Proc. IEEE*, vol. 92, no. 7, pp. 1122–1137, Jul. 2004.

[77] T. Batista Napotnik, M. Reberšek, P. T. Vernier, B. Mali, and D. Miklavčič, "Effects of high voltage nanosecond electric pulses on eukaryotic cells (in vitro): A systematic review," *Bioelectrochemistry*, vol. 110, pp. 1–12, Aug. 2016.

[78] P. T. Vernier, Y. Sun, and M. A. Gundersen, "Nanoelectropulse-driven membrane perturbation and small molecule permeabilization," *BMC Cell Biol.*, vol. 7, no. 1, Dec. 2006, Art. no. 37.

[79] A. G. Pakhomov, J. F. Kolb, J. A. White, R. P. Joshi, S. Xiao, and K. H. Schoenbach, "Long-lasting plasma membrane permeabilization in mammalian cells by nanosecond pulsed electric field (nsPEF)," *Bioelectromagnetics*, vol. 28, no. 8, pp. 655–663, Dec. 2007.

[80] Z. Vasilkoski, A. T. Esser, T. R. Gowrishankar, and J. C. Weaver, "Membrane electroporation: The absolute rate equation and nanosecond time scale pore creation," *Phys. Rev. E, Stat. Phys. Plasmas Fluids Relat. Interdiscip. Top.*, vol. 74, no. 2, Aug. 2006, Art. no. 021904.

[81] O. M. Nesin, O. N. Pakhomova, S. Xiao, and A. G. Pakhomov, "Manipulation of cell volume and membrane pore comparison following single cell permeabilization with 60- and 600-ns electric pulses," *Biochimica Biophysica Acta (BBA)-Biomembranes*, vol. 1808, no. 3, pp. 792–801, Mar. 2011.

[82] W. R. Rogers, J. H. Merritt, J. A. Comeaux, C. T. Kuhnel, D. F. Moreland, D. G. Teltschik, J. H. Lucas, and M. R. Murphy, "Strength-duration curve for an electrically excitable tissue extended down to near 1 nanosecond," *IEEE Trans. Plasma Sci.*, vol. 32, no. 4, pp. 1587–1599, Aug. 2004.

[83] A. G. Pakhomov, I. Semenov, M. Casciola, and S. Xiao, "Neuronal excitation and permeabilization by 200-ns pulsed electric field: An optical membrane potential study with FluoVolt dye," *Biochimica-Biophysica Acta (BBA)-Biomembranes*, vol. 1859, no. 7, pp. 1273–1281, Jul. 2017.

[84] C. Chen, S. W. Smye, M. P. Robinson, and J. A. Evans, "Membrane electroporation theories: A review," *Med. Biol. Eng. Comput.*, vol. 44, nos. 1–2, pp. 5–14, Mar. 2006.

[85] R. P. Joshi and K. H. Schoenbach, "Electroporation dynamics in biological cells subjected to ultrafast electrical pulses: A numerical simulation study," *Phys. Rev. E, Stat. Phys. Plasmas Fluids Relat. Interdiscip. Top.*, vol. 62, no. 1, pp. 1025–1033, Jul. 2000.

[86] J. C. Neu and W. Krassowska, "Asymptotic model of electroporation," *Phys. Rev. E, Stat. Phys. Plasmas Fluids Relat. Interdiscip. Top.*, vol. 59, no. 3, pp. 3471–3482, Mar. 1999.

[87] A. L. Hodgkin and A. F. Huxley, "Propagation of electrical signals along giant nerve fibres," *J. Physiol.*, vol. 117, pp. 177–183, Jan. 1952.

[88] W. Milestone, C. Baker, A. L. Garner, and R. P. Joshi, "Electroporation from mitochondria to cell clusters: Model development toward analyzing electrically driven bioeffects over a large spatial range," *J. Appl. Phys.*, vol. 133, no. 24, Jun. 2023, Art. no. 244701.
[89] E. Goldberg, C. Suárez, M. Alfonso, J. Marchese, A. Soba, and G. Marshall, "Cell membrane electroporation modeling: A multiphysics approach," *Bioelectrochemistry*, vol. 124, pp. 28–39, Dec. 2018.
[90] F. Guo, K. Qian, L. Zhang, X. Liu, and H. Peng, "Multiphysics modelling of electroporation under uni- or bipolar nanosecond pulse sequences," *Bioelectrochemistry*, vol. 141, Mar. 2021, Art. no. 107878.
[91] X.-Z. Hao, Y.-Z. Xie, J. Guo, and W.-C. Xie, "A 3-D multi-physics modeling of electroporation excited by a single pulse," *IEEE Trans. Dielectr. Electr. Insul.*, vol. 30, no. 2, pp. 546–555, Apr. 2023.
[92] M. Essone Mezeme, G. Pucihar, M. Pavlin, C. Brosseau, and D. Miklavčič, "A numerical analysis of multicellular environment for modeling tissue electroporation," *Appl. Phys. Lett.*, vol. 100, no. 14, Apr. 2012, Art. no. 143701.
[93] M. Kumar and A. Mishra, "Multiphysics analysis of reversible electroporation and electrodeformation of cervical cells using a nanosecond pulse generator," *IEEE Trans. Plasma Sci.*, vol. 51, no. 2, pp. 534–543, Feb. 2023.
[94] F. Guo, K. Qian, H. Deng, and X. Li, "Multiphysics analysis of nsPEF induced electrodeformation in a dispersive cell model," *Appl. Phys. Lett.*, vol. 118, no. 8, Feb. 2021, Art. no. 083701.
[95] K. Gajula, R. Gupta, and B. Rai, "Multiscale modeling of skin electroporation," *Langmuir*, vol. 36, no. 24, pp. 6651–6660, Jun. 2020.
[96] R. L. Weinert, M. A. Knabben, E. M. Pereira, C. E. Garcia, and A. Ramos, "Dynamic electroporation model evaluation on rabbit tissues," *Ann. Biomed. Eng.*, vol. 49, no. 9, pp. 2503–2512, Sep. 2021.
[97] A. M. Dagro, J. W. Wilkerson, T. P. Thomas, B. T. Kalinosky, and J. A. Payne, "Computational modeling investigation of pulsed high peak power microwaves and the potential for traumatic brain injury," *Sci. Adv.*, vol. 7, no. 44, Oct. 2021, Art. no. eabd8405.
[98] B. Mercadal, P. T. Vernier, and A. Ivorra, "Dependence of electroporation detection threshold on cell radius: An explanation to observations non compatible with Schwan's equation model," *J. Membrane Biol.*, vol. 249, no. 5, pp. 663–676, Oct. 2016.
[99] T. Kotnik, D. Miklavčič, and T. Slivnik, "Time course of transmembrane voltage induced by time-varying electric fields—A method for theoretical analysis and its application," *Bioelectrochem. Bioenergetics*, vol. 45, no. 1, pp. 3–16, Mar. 1998.
[100] W. Milestone, Q. Hu, A. M. Loveless, A. L. Garner, and R. P. Joshi, "Modeling coupled single cell electroporation and thermal effects from nanosecond electric pulse trains," *J. Appl. Phys.*, vol. 132, no. 9, Sep. 2022, Art. no. 094701.
[101] S. Talele, P. Gaynor, M. J. Cree, and J. van Ekeran, "Modelling single cell electroporation with bipolar pulse parameters and dynamic pore radii," *J. Electrostatics*, vol. 68, no. 3, pp. 261–274, Jun. 2010.
[102] A. G. Pakhomov, E. Gianulis, P. T. Vernier, I. Semenov, S. Xiao, and O. N. Pakhomova, "Multiple nanosecond electric pulses increase the number but not the size of long-lived nanopores in the cell membrane," *Biochimica-Biophysica Acta (BBA)-Biomembranes*, vol. 1848, no. 4, pp. 958–966, Apr. 2015.
[103] W. Frey, J. A. White, R. O. Price, P. F. Blackmore, R. P. Joshi, R. Nuccitelli, S. J. Beebe, K. H. Schoenbach, and J. F. Kolb, "Plasma membrane voltage changes during nanosecond pulsed electric field exposure," *Biophys. J.*, vol. 90, no. 10, pp. 3608–3615, May 2006.
[104] R. P. Joshi, Q. Hu, R. Aly, K. H. Schoenbach, and H. P. Hjalmarson, "Self-consistent simulations of electroporation dynamics in biological cells subjected to ultrashort electrical pulses," *Phys. Rev. E, Stat. Phys. Plasmas Fluids Relat. Interdiscip. Top.*, vol. 64, no. 1, Jun. 2001, Art. no. 011913.
[105] T. Kotnik, L. Rems, M. Tarek, and D. Miklavčič, "Membrane electroporation and electropermeabilization: Mechanisms and models," *Annu. Rev. Biophys.*, vol. 48, no. 1, pp. 63–91, May 2019.
[106] T. Kotnik, G. Pucihar, and D. Miklavčič, "Induced transmembrane voltage and its correlation with electroporation-mediated molecular transport," *J. Membrane Biol.*, vol. 236, no. 1, pp. 3–13, Jul. 2010.
[107] T. Kotnik and D. Miklavčič, "Theoretical evaluation of voltage inducement on internal membranes of biological cells exposed to electric fields," *Biophys. J.*, vol. 90, no. 2, pp. 480–491, Jan. 2006.
[108] S. Nath, K. P. Sinha, and R. M. Thaokar, "Development of transmembrane potential in concentric spherical, confocal spheroidal, and bispherical vesicles subjected to nanosecond-pulse electric field," *Phys Rev. E*, vol. 101, Feb. 2020, Art. no. 062407.
[109] V. Novickij, A. Balevičiūtė, P. Ruzgys, S. Šatkauskas, J. Novickij, A. Zinkevičienė, and I. Girkontaitė, "Sub-microsecond electrotransfection using new modality of high frequency electroporation," *Bioelectrochemistry*, vol. 136, Dec. 2020, Art. no. 107594.
[110] T. Potočnik, D. Miklavčič, and A. Maček Lebar, "Gene transfer by electroporation with high frequency bipolar pulses in vitro," *Bioelectrochemistry*, vol. 140, Aug. 2021, Art. no. 107803.
[111] K. N. Aycock, Y. Zhao, M. F. Lorenzo, and R. V. Davalos, "A theoretical argument for extended interpulse delays in therapeutic high-frequency irreversible electroporation treatments," *IEEE Trans. Biomed. Eng.*, vol. 68, no. 6, pp. 1999–2010, Jun. 2021.
[112] S. D. Dynako, A. M. Loveless, and A. L. Garner, "Sensitivity of modeled microscale gas breakdown voltage due to parametric variation," *Phys. Plasmas*, vol. 25, no. 10, Oct. 2018, Art. no. 103505.
[113] Y. Feldman, I. Ermolina, and Y. Hayashi, "Time domain dielectric spectroscopy study of biological systems," *IEEE Trans. Dielectr. Electr. Insul.*, vol. 10, no. 5, pp. 728–753, Oct. 2003.
[114] A. L. Garner, G. Chen, N. Chen, V. Sridhara, J. F. Kolb, R. J. Swanson, S. J. Beebe, R. P. Joshi, and K. H. Schoenbach, "Ultrashort electric pulse induced changes in cellular dielectric properties," *Biochem. Biophys. Res. Commun.*, vol. 362, no. 1, pp. 139–144, Oct. 2007.

AMANDA M. LOVELESS (Member, IEEE) received the B.S. and M.S. degrees in nuclear engineering from Purdue University, in 2015 and 2017, respectively, and the Ph.D. degree in nuclear engineering, in 2020.

She is currently a Research Scientist with the School of Nuclear Engineering, Purdue University. Her research interests include theoretical studies of gas breakdown, electron emission, and bioelectric phenomena.

Dr. Loveless received the 2016 Krauss Scholarship from Purdue University, the 2016 IEEE Dielectrics and Electrical Insulation Society (DEIS) Graduate Fellowship, the 2017 IEEE Nuclear and Plasma Sciences Society (NPSS) Graduate Scholarship, the 2018 Igor Alexeff Outstanding Student in Plasma Science Award, and Three Directed Energy Professional Society (DEPS) Scholarships. She also won the First Place for "Best Student Paper" at the 2016 International Conference on Plasma Science (ICOPS) and the 2016 Electrostatic Society of America (ESA) Annual Meeting. She also received the 2020 Purdue College of Engineering (COE) Outstanding Graduate Research Award for the School of Nuclear Engineering. She is currently an elected member of the (2023–2026) IEEE Pulsed Power Science & Technology (PPST) Committee.

SAMUEL J. WYSS (Graduate Student Member, IEEE) received the B.S. degree in nuclear engineering from Purdue University, West Lafayette, IN, USA, in 2023, where he is currently pursuing the Graduate degree in nuclear engineering.

His research interests include computational physics and bioelectrics.

WILLIAM MILESTONE received the B.S. degree in applied physics and the M.S. and Ph.D. degrees in electrical engineering from Texas Tech University, Lubbock, TX, USA, in 2019, 2021, and 2023, respectively. He is currently a Senior Scientist with Nanohmics, Inc., Austin, TX, USA.

RAVI P. JOSHI (Fellow, IEEE) received the B.Tech. and M.Tech. degrees in electrical engineering from IIT Bombay, India, and the Ph.D. degree from Arizona State University, Tempe, AZ, USA, in 1983, 1985, and 1988, respectively. He is currently a Full Professor with Texas Tech University, Lubbock, TX, USA. He has authored more than 210 journal publications. His current research interests include the modeling of charge transport, electric breakdown, nonequilibrium phenomena, semiconductor physics, and bioelectrics. He is a Licensed Professional Engineer in Texas. He is also a fellow of the Institute of Physics (FInstP), Institution of Engineering and Technology (FIET), and the Institution of Electronics & Telecommunication Engineers; and an IEEE Distinguished Lecturer. He also received the 2017 IEEE-NPSS Merit Award and the 2022 IEEE-IPMHVC Dunbar Award. He has served as a Guest Editor for five special issues for IEEE TRANSACTIONS ON PLASMA SCIENCE. He is also a senior editor.

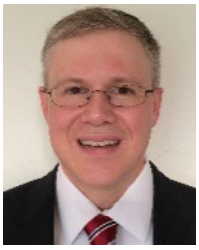

ALLEN L. GARNER (Senior Member, IEEE) received the B.S. degree (Hons.) in nuclear engineering from the University of Illinois at Urbana–Champaign, in 1996, the M.S.E. degree in nuclear engineering from the University of Michigan, Ann Arbor, in 1997, the M.S. degree in electrical engineering from Old Dominion University, Norfolk, VA, USA, in 2003, and the Ph.D. degree in nuclear engineering from the University of Michigan, in 2006.

From December 1997 to December 2003, he was an active duty Naval officer onboard the USS Pasadena (SSN 752) and as an instructor with the Prospective Nuclear Engineering Officer Course, Submarine Training Facility, Norfolk. From 2006 to 2012, he was an Electromagnetic Physicist with the GE Global Research Center, Niskayuna, NY, USA. In August 2012, he joined the School of Nuclear Engineering, Purdue University, West Lafayette, IN, USA, where he is currently a Professor and the Undergraduate Program Chair. He is also a Captain with the Navy Reserves and the Commanding Officer of NR SurgeMain Puget Sound Naval Shipyard Kitsap, Bremerton, WA, USA. His research interests include electron emission, gas breakdown, high-power microwaves, and biomedical applications of pulsed power and plasmas.

Prof. Garner is a Licensed Professional Engineer in Michigan. He is a member of the IEEE International Power Modulator and High Voltage Conference (IPMHVC) Executive Committee and the Dielectrics and Electrical Insulation Society Administrative Committee. He received the 2016 IEEE Nuclear and Plasma Sciences Early Achievement Award, Two Meritorious Service Medals, the Navy and Marine Corps Commendation Medal, and Five Navy and Marine Corps Achievement Medals. He served as the Technical Program Chair for the 2016 IEEE IPMHVC, a Treasurer for the 2018 IEEE IPMHVC, and the Technical Program Chair for the 2022 IEEE IPMHVC. He is the General Conference Chair of the 2024 IEEE IPMHVC.